PONTIFICIA UNIVERSIDAD CATOLICA DE CHILE

ESCUELA DE INGENIERIA

CHARACTERIZATION AND EFFECTS OF FREEZING PRIOR TO FRYING ON THE MICROSTRUCTURE AND TRANSPORT PHENOMENA OF FORMULATED PRODUCTS

MATHIAS CRUZ BUSSE

Thesis submitted to the Office of Research and Graduate Studies in partial fulfillment of the requirements for the Degree of Master of Science in Engineering

Advisor:

PEDRO ALEJANDO BOUCHON AGUIRRE

Santiago de Chile, August, 2014

PONTIFICIA UNIVERSIDAD CATOLICA DE CHILE
ESCUELA DE INGENIERIA

CHARACTERIZATION AND EFFECTS OF FREEZING PRIOR TO FRYING ON THE MICROSTRUCTURE AND TRANSPORT PHENOMENA OF FORMULATED PRODUCTS

MATHIAS CRUZ BUSSE

Members of the Committee:

PEDRO BOUCHON

LORETO VALENZUELA

KUMAR MALLIKARJURAN

GONZALO PIZARRO

Thesis submitted to the Office of Research and Graduate Studies in partial fulfillment of the requirements for the Degree of Master of Science in Engineering

Santiago de Chile, August, 2014

ACKNOWLEDGEMENTS

First of all I would like to thank Dr. Pedro Bouchon for all his guidance, his patience and all the knowledge he transferred to me. I am especially thankful for all the discussions trying to make each other understand something, it was the most valuable learning of my thesis.

I would also like to express my gratitude to all the staff working at the Department of Chemical and Bioprocess Engineering, especially to Mrs. María Inés Valdebenito, for her invaluable help when doing paperwork. I must also thank my colleague Carolina Moreno, for all her advice and help. Without both, I would have been lost.

My special gratitude goes to my family. My parents support allowed me to complete this project. My brothers and sisters willingness to always listen to me and make fun about my thesis, made the day-to-day easier.

I would like to express my biggest gratitude to some special friends. To Sergio and Constanza, for always being there every day, for always listening and for making every day of this process extraordinary. I must also thank Francisca, for always understanding and be willing to talk. For being the only person who once visited me.

Very special thanks to the financial support from Fondecyt proyect number 1131083 and Anillo Project ACT-1105/2012 “Healthy Food Matrix Design”.

I would also like to express my gratitude to Armin van Buuren and his radio show A State of Trance, for being the best company in the long hours working at the laboratory.

Last, but not least, I want to thank God, for the opportunity he gave me to accomplish my dreams. The people I knew and surrounded me all this time. Thanks for a year full of grace.

GENERAL INDEX

TABLE INDEX

FIGURE INDEX

ABSTRACT

Formulated products are getting importance in the snack industry. In fried products, these might be an option for the production of snacks with reduced oil content and enhanced properties. Oil absorption has been suggested as the most critical quality parameter in fried snacks and several studies have shown that it is a surface phenomenon, where drainage and suction of oil compete to determine the final oil content. Freezing of foods is one of the most common ways to preserve them. Slow freezing rates give time and mobility to water to form big ice crystals, which disrupt the food microstructure, meanwhile fast freezing rates freeze water so abruptly that ice crystals are hardly formed.

Accordingly, the hypothesis of this thesis stated that the rate of freezing affects the microstructure of raw dough and therefore the developed microstructure during deep-fat frying and the associated oil absorption capacity of the matrix. Consequently, the objective of this thesis was to understand the effect of the freezing rate on the microstructure of gluten and starch formulated dough during deep-fat frying and associated transport phenomena, particularly oil absorption.

Products were formulated ensuring 10% gluten (d.b.), 90% starch (d.b.) and a water content of 70% (d.b.). Two different thicknesses were analyzed: 1 cm and 0.5 cm in 10-cm diameter discs. Slow freezing rates were carried in a conventional freezer; meanwhile fast freezing was carried in an air blast freezer. Afterwards discs were deep fat fried in high oleic sunflower oil at 170°C until reaching three different moistures 50%, 40% and 30% d.b. Temperature profiles of the discs were measured during the cooling and frying processes. In addition, oil distribution within the crust was analyzed non-invasively using confocal laser scanning microscopy.

The period of time that the sample remained at the freezing plateau increased significantly when the freezing process was slowed down, confirming that different freezing rates were actually achieved. It was observed that fast-frozen products melted faster, had higher freezing rates and developed more crust than slow-frozen products. With respect to the effect of freezing on oil absorption, it was observed that slow

freezing decreased significantly oil-uptake during deep-fat frying, which was attributed to the possible collapse of the inner structure. Total oil measurement was divided into penetrated and surface oil. Penetrated oil had the same behavior as total oil did, mainly because it represented over 80% of total oil content. No significant differences between thin and thick products were observed. Overall, differences in total oil absorption between thin and thick products were due to surface oil fraction. These differences could be maybe attributed to differences in surface roughness, which may reduce oil drainage in thin samples, but further studies are needed to elucidate this hypothesis.

Overall, this works sets-up an initial basis to understand the relationship between freezing and deep-fat frying, and thus, represent a novel contribution in the field of food product design, to meet new consumer's demands.

RESUMEN

La congelación es un proceso sumamente importante debido a su capacidad para conservar los alimentos. El objetivo de este trabajo es entender el efecto que tienen distintas tasas de congelación en la microestructura de productos congelados, especialmente en la absorción de aceite. Se prepararon matrices con un 10% (b.s.) de gluten y 90% (b.s.) de almidón, asegurando un contenido de 70% (b.s.) de humedad). Se formaron discos de 10cm de diámetro y espesores de 10 y 5mm, que luego se congelaron a distintas tasas. Inmediatamente después los discos fueron fritos hasta alcanzar pérdidas de humedad de 20, 30 y 40%. Se midieron perfiles de temperatura del proceso en distintas posiciones. Distintas tasas de congelación aseguraron distintas microestructuras, manifestadas en: mayores tasas de calentamiento, de formación de costra y pérdida de humedad en congelamiento rápido. La congelación lenta disminuyó significativamente la absorción de aceite, probablemente debido a la formación de grandes cristales de hielo, los cuales podrían inducir un colapso de la estructura al derretirse. La cantidad de aceite que penetra la estructura es proporcional al espesor, manteniendo la relación de aceite/sólidos, demostrando así que la penetración de aceite es un fenómeno superficial.

1 INTRODUCTION

In recent years the market of foods has suffered a revolution. Consumers are more demanding. They desire to eat healthier and safer foods, with desirable organoleptic properties, but they are not willing to invest long periods of time if food preparation. Due to this, food engineering faces a major challenge, which also an opportunity, not only to produce better foods, but to adequate them to the new living styles. This has led researchers to develop convenient ready to eat food, with unique sensory attributes. Frying of foods has been widely studied because of the unique properties that it confers to foods. On the other hand, freezing of foods is a fundamental process in food technology, because of its unique properties to preserve food. However, the relationship and sequence between freezing and frying has not yet been studied thoroughly, which in turn could lead to a better understanding of convenient-food preparation.

1.1 Food microstructure

A very common way to create novel structures is via product formulation. Different ingredients and processes are mixed in order to get specific functional characteristics. It is critical to understand the properties of the structural elements that may be used, that is, the food building blocks. Their functionality, their response during/after processing, as well as their interactions, are the key factors to understand the behavior of foods. The most common building blocks in snack and fried product matrixes are gluten, starch, modified starches (e.g. pregelatinized, acethylated, crosslinked, hydroxypropilated) and potato flakes/granules (Grandison, 2012), as well as water and air.

Gluten is a protein that gives the structural component to formulated matrixes, because of its two main constituents: glutenins and gliadins. Glutenins are multichained high molecular weight proteins, which exhibit pronounced resiliency but little extensibility, and therefore, appear to provide the elastic properties of gluten. Gliadins consist of some 50 single-chained proteins of relatively low molecular weight. They are

notably extensible and sticky, providing the extensibility and cohesive properties of gluten (Veraverbeke & Delcour, 2002). Starch is the most common carbohydrate polymer in food (Eliasson & Gudmundsson, 1996). Starch granules are insoluble in water at room temperature. In the presence of adequate temperature and water, the crystalline structure is disrupted, allowing the amorphous regions to become more accessible to absorb water and swell, a process known as gelatinization.

In order to characterize how these food building blocks give their properties to foods we come along to microstructural characterization. In foods, most of the critical constituents and transformations, and associated properties occur in a scale that is below 100 μm and cannot be seen without appropriate tools. Different microscopy techniques have allowed researchers to understand the microstructure of food materials, such as light microscopy, transmission electron microscopy or scanning electron microscopy (Aguilera, 2005). However, a thoughtful equilibrium between sample preparation and capacity of observation must be defined, in order to avoid artefacts inclusion, which may distort measurements. Another technique that may be used is confocal laser scanning microscopy (CLSM). This technique allows optical sectioning to be carried out using a laser beam, avoiding physical damage of the specimen. In relation to frying, CLSM has been used to study oil location directly in fried potato chips with minimal intrusion (Bouchon et al., 2003; Pedreschi et al., 1999). This was achieved by frying the food directly in an oil bath that contained a heat stable fluorochrome (Nile Red), without further preparation, transferring the sample under the lenses of a CLSM. Recently, Moreno and Bouchon (2013) used this technique to study oil absorption and structural changes in formulated products. Microstructural characterization may be also used to understand macrostructural properties of foods and transport phenomena, as shown by Moreno (2012), who correlated key microstructural properties to oil absorption kinetics and texture.

1.2 Deep fat frying

Deep-fat frying is the process of cooking of foods by immersing them in an edible oil or fat at a temperature well above the boiling point of water, at the operating

pressure, to induce fast dehydration. Oil content is one of the most important quality parameters of fried food, which is incompatible with recent consumer trends towards healthier food and low fat products (Bouchon & Pyle, 2004). In order to reduce oil content of fried foods, oil penetration mechanisms must be understood, so that oil migration into the structure can be minimized. Regarding oil absorption kinetics, it has been suggested that most of the oil is absorbed after removing the product from the oil bath, since the vigorous escape of water vapor would prevent oil penetration during most of the immersion period. As a result, oil absorption would result from the competition between drainage and suction into the porous crust once the food is removed from the oil (Bouchon et al., 2003). Moreno et al. (2010), showed though that in laminated gluten based products oil penetration has a greater degree of penetration during the immersion period, than in non-gluten products.

Despite the progress that has been made, the oil adsorption process is not fully understood, and it is difficult to predict the final oil content of fried products. Studies have shown that oil absorption is a surface-related phenomenon. Consequently oil uptake mainly occurs in the outer layers of the product, that is, the crust region (Bouchon & Aguilera, 2001; Bouchon et al., 2003; Moreira et al., 1997; Ufheil & Escher, 1996). The importance of microstructure in deep-fat frying has been emphasized when studying oil absorption mechanisms (Dueik & Bouchon, 2011). Fried-food microstructure is a combination of both surface and inner properties, which play different but key roles in oil absorption. Surface topography has a major role in oil drainage during post-frying cooling, whereas the crust inner structure defines product permeability and the available space for oil deposition (Moreno et al., 2010). In fact, the competition between surface drainage and oil penetration during cooling, which may well be mediated by capillary forces, has been found to determine the final oil content of the product (Bouchon et al., 2003). Previous studies have pointed out that the micro-structure of the crust region, which is formed while the food is been cooked in the frying oil, is the most important product-related determinant of the final oil uptake into the product (Bouchon & Aguilera, 2001; Pinthus et al., 1995). Accordingly Bouchon et al.

(2003), were able to identify three different oil fractions as a consequence of the different mechanisms, that is: i) structural oil (STO), which represents the amount of oil absorbed during frying, ii) penetrated surface oil (PSO), which represents the amount of oil suctioned into the food during cooling, following its removal from the fryer and iii) surface oil (SO), that is, the oil that remains on the surface (Bouchon et al., 2003). Figure 1.1 shows a diagram of the three different oil fractions.

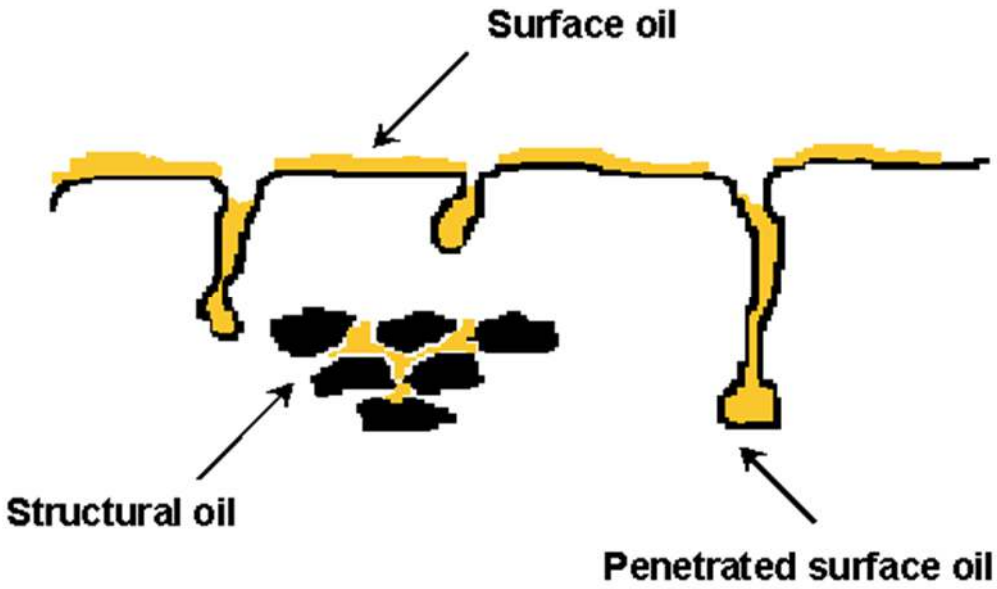

Figure 1.1: Diagram of the three oil fractions absorbed during the frying process (Bouchon et al., 2003).

Researchers have developed different techniques to reduce oil content. It has been shown that gluten based products are less permeable to oil, as higher gluten content resulted in lower oil uptake (Gazmuri & Bouchon, 2009; Moreno & Bouchon, 2013). Various pre-frying treatments attempt to reduce the oil absorption by reducing surface permeability. This can be achieved through edible film coating or direct blend modification, as in formulated products, using hydrocolloids such as methylcellulose, hydroxypropyl methylcellulose, long fiber cellulose, corn zein, starch, and modified starch, among others (Bouchon & Pyle, 2004; □□□í□ ., 2002; Mellema, 2003). Also, pre-dehydration has shown to be an effective pre-treatment to reduce the oil content

upon frying, probably due to the changes induced to the surface of the food, which reduce surface permeability. Microwave, hot-air treatment, and baking have resulted in a significant reduction in oil content in different products (Gamble et al., 1987; Moreno & Bouchon, 2008). Some pre-drying treatments as freeze- or osmotic-drying have demonstrated to have an inverse effect, increasing oil absorption, mainly because of the higher porosity of the external structure that reduces the resistance to oil absorption (Moreno & Bouchon, 2008).

1.3 Freezing principles

Freezing is a highly important process, because of its high capacity to preserve food. However, important microstructural transformations related to ice crystal formation and their growth occur in the process of freezing; therefore, the importance of understanding how freezing is carried out. Ice crystallization will only occur if a supersaturated state is reached, that is, if the temperature is constantly below the freezing point of the matrix so that a driving force for crystallization always remains during freezing, exciding equilibrium (Hartel, 2001). In the presence of other components, such as small molecules, carbohydrates and proteins, among others, the freezing point of water will decrease. Freezing consists of three stages, i.e., cooling the product to its freezing point, removing the latent heat of crystallization and finally cooling the product to the final storage temperature (Kiani & Sun, 2011). Figure 1.2 schematically shows typical curves of fast and slow freezing for foods: first the initial cooling until reaching point *a*, which is the ice crystallization temperature, then the trajectory from point *b* to *c* where the latent heat is removed, a process that takes considerably longer in slow freezing and the final cooling up to the target temperature. In the case of slow freezing temperature does not drop during the freezing plateau, but fast freezing is that abrupt, that temperature might drop.

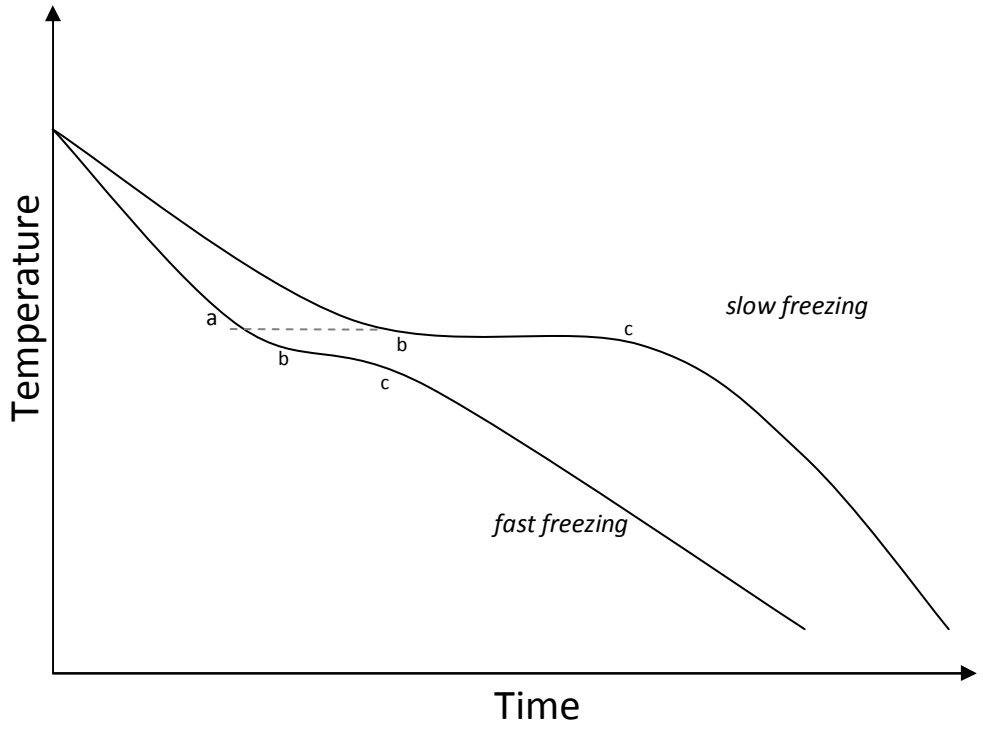

Figure 1.2: Typical cooling curves of foods. a: Ice crystallization temperature, b: equilibrium or initial freezing point, c: end of freezing. (Adapted from Rahman, 2008)

Ice morphology is an important factor affecting the quality of frozen foods and is determined by the freezing conditions (Petzold & Aguilera, 2009). At low freezing rates there is time and mobility for ice crystals to accommodate in disk morphologies, so that the water molecules will arrange in hexagonal units (Petzold & Aguilera, 2009; Wathen et al., 2004). This may induce an important collapse of the structure. On the other hand, higher freezing rates may be so abrupt that there may not even allow crystal growth due to restricted mobility, affecting the morphology of ice crystals and causing the disk morphology to change into other forms like perturbed disk, dendrite, needle, or platelet (Petzold & Aguilera, 2009; Tressler et al., 1968). As a consequence, at atmospheric pressures faster freezing rates produce smaller and homogeneous arrangements and slower freezing rates produce larger and more heterogeneous crystals (Kiani & Sun, 2011).

To determine when a food is frozen is not an easy task, the process is complex and it is very difficult to freeze the total amount of water. At the end of the freezing process the centre of the food is often hotter than its surface. The temperature at which water freezes diminishes in solutions (to even -40°C) and if the sample is not homogeneous there might be different freezing points, which is often the case in food matrices. Therefore, most of the water solidifies in proximities of the 0°C and at -4°C about 73% of the total water is already in solid state (Plank, 1963). Freezing of water results in temperature-dependent freeze concentration as ice crystals are separated from dissolved and other solids as dispersed ice in a continuous, unfrozen phase. This unfrozen phase has a temperature and composition-dependent water plasticization behavior as the plasticizing unfrozen water content changes with temperature, and concomitant changes in the ice and unfrozen water contents take place. The maximally freeze-concentrated state can be formed in the vicinity of the glass transition of the maximally freeze-concentrated solute phase. Glass formation in freeze-concentrated solutions and food systems occurs as a result of (a) the separation of ice in a dispersed solid phase, and (b) the decreased temperature and increased viscosity of the unfrozen phase. As the freeze-concentrated phase approaches a high solids content and high viscosity, the rate of crystallization of water is reduced. At some level of freeze-concentration and increasing viscosity, ice formation ceases (Roos, 2010).

For an infinite slab which is cooled from both sides, freezing time can be modeled by Plank's equation, which only describes the phase change period of the freezing process. Some suppositions have to be made:

(1) Heat transfer is mono-dimensional, only loosing heat from the two faces.

(2) The initial temperature is uniform and is at the freezing point of the material.

(3) The temperature of the freezing medium (air) is constant.

(4) Latent heat is removed at a constant temperature.

(5) Properties of food above and below the freezing point are different but constant.

(6) Heat transfer inside the food is by conduction.

If the following variables are considered:

$t\ [s]$: $is\ the\ time$

$Q\ [J/s]$: $is\ the\ heat\ flow\ to\ remove$

$A[m^2]$: $is\ the\ area\ exposed\ to\ the\ cooling\ medium$

$\rho\ [J/kg]$: $is\ the\ latent\ heat\ of\ the\ object$

$\Delta\ [kg/m^3]$: $is\ the\ density\ of\ the\ object$

$Ta\ [°C]$: $is\ the\ temperature\ of\ the\ air$

$Ts\ [°C]$: $is\ the\ temperature\ of\ the\ slab.$

$\theta[°C]$: $is\ the\ temperature\ difference\ between\ the\ freezing$
$temperature\ and\ the\ cooling\ medium$

$\delta\ [m]$: $is\ the\ thickness\ of\ the\ frozen\ layer\ formed$

$h\ [m]$: $is\ the\ thickness\ of\ the\ slab$

$a\ [J/(m^2 s°C)]$: $is\ the\ thermal\ transport\ coefficient\ between$
$the\ slab\ surface\ and\ the\ cooling\ medium$

$\lambda\ [J/(ms°C)]$: $is\ the\ thermal\ transport\ coefficient\ inside\ the\ slab$

and a differential balance is carried out according to the slab depicted in Figure 1.3, the following development may be obtained.

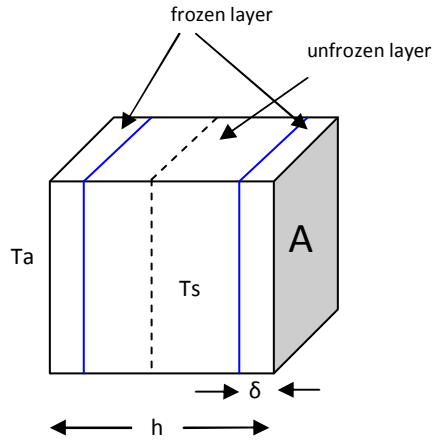

Figure 1.3: Differential heat balance for the slab, for the frozen and unfrozen layer.

Water undergoes a phase change into ice at the freezing front. The rate at which latent heat is removed at the freezing front is:

$$Q = A\,\rho\,\Delta\,\frac{d\delta}{dt} \quad (1)$$

The resistance to heat transfer (R_H) is the sum of the convective and conductive resistance to the heat removal: $R_H = \frac{1}{\alpha} + \frac{\delta}{\lambda}$

The heat transfer can be calculated as:

$$Q = A\frac{Ts - Ta}{R_H} = A\frac{Ts - Ta}{\left(\frac{1}{\alpha} + \frac{\delta}{\lambda}\right)} \quad (2)$$

If both equations are equalized:

$$A\,\rho\,\Delta\,\frac{d\delta}{dt} = A\,\frac{\theta}{\left(\frac{1}{\alpha} + \frac{\delta}{\lambda}\right)}$$

And then rearranged, equation (3) can be obtained:

$$dt = \frac{\rho\,\Delta}{\theta}\,\frac{d\delta}{\left(\frac{1}{\alpha} + \frac{\delta}{\lambda}\right)} \quad (3)$$

Separating variables, the expression can be integrated between t=0 and the time needed (t_o) freeze the center of the slab (h/2), to obtain:

$$t_o = \frac{\rho\,\Delta}{\theta}\left(\frac{h}{2a} + \frac{h^2}{8\lambda}\right) \quad (4)$$

Accordingly, the freezing rate may be defined as:

$$w = \frac{d\delta}{dt} \quad (5)$$

Where w (m/h) is the speed at which the frozen layer is formed. It is an important parameter, because it determines the crystalline structure formed and therefore the microstructure that develops in a frozen food. This rate is not constant, it can vary along the layers of food increasing or decreasing from the surface to the center (Plank, 1963). It changes, because ice transfers heat faster than water, so the inner part of the foods will freeze slower than the parts that are already frozen. This can be seen through equation (3):

$$w = \frac{d\delta}{dt} = 1/\frac{\rho\,\Delta}{\theta}\left(\frac{1}{a} + \frac{\delta}{\lambda}\right) = \frac{\theta}{\rho\,\Delta}\frac{1}{1/a + \delta/\lambda} \quad (6)$$

Consequently freezing rate diminishes continuously from the surface to the center, independent of the thickness of the slab. Applications of this and other models have practical complications, as heat transfer coefficients are hard to estimate, with typical uncertainties of ±10-20% (Delgado & Sun, 2001). Empirical approaches are thereby a good alternative, as suggested by Rahman et al. (2002) who used the cooling curve and plotted temperature *versus* time to determine the end point of freezing. To establish whether a freezing rate is fast or slow will depend on the food matrix. Changes in the food microstructure could be minimal even with very different rates in some food structures as meat. For this reason, it is often very hard to establish a critical point over which a freezing rate is considered to be fast. For food matrixes composed mainly of starch, the point over which a freezing rate could be considered fast ranges between 1.5 and 2 cm/h (Plank, 1963; Rahman, 2007; Sun, 2011).

Other models have also been developed, which make suppositions that make the problem more complex. While Planck's model assumes quasi-steady state heat transfer, the Neumann's model is more generally applicable and is based on unsteady state conduction through frozen and unfrozen layers. Because this model considers

temperature variation along the food it can be useful to solve real problems, meanwhile Planck's model is better to understand the freezing phenomena than for modeling purposes. The Neumann's model establishes the position of the freezing front as:

$$x = 2N\sqrt{at} \quad (7)$$

Where x (m) is the position of the freezing front, *t (s)* is time, a_1 *(m²/s)* is the thermal diffusivity of the frozen zone, and N represents the Neumann dimensionless characteristic number (Pardo & Niranjan, 2006). Basic heat equations involved in Neumann's model are presented in Table 1.1.

Table 1.1: Basic heat equations involved in Neumann's model (Pardo & Niranjan, 2006).

	Frozen layer	***Liquid layer***
Conservation equation	$\frac{\partial T_1}{\partial t} = a_1 \frac{\partial^2 T_1}{\partial x^2}, 0 < x < s$	$\frac{\partial T_2}{\partial t} = a_2 \frac{\partial^2 T_2}{\partial x^2}, s < x < x_t$
Initial conditions and	$T_1 = T_t\ , x = 0\ , t > 0$	$T_2 = T_0\ for\ all\ x\ , t = 0$
boundary conditions	$T_1 = T_m\ , x = s\ , t > 0$	$T_2 = T_0\ , x \to \infty\ , t > 0$
		$T_2 = T_m\ , x = s\ , t > 0$
At the ice front	$-K_1 \frac{\partial T_1}{\partial x} + K_2 \frac{\partial T_2}{\partial x} + \rho_1 \Delta H_f \frac{\partial s}{\partial t}\ , x = s$	

A further model, the Cleland Model estimates freezing times of food samples based on the following assumptions: (a) the conditions of the surrounding are constant, (b) the sample is found initially at a uniform temperature, (c) the final temperature has a fixed value and (d) Newton's cooling law describes the heat transfer at the surface (Pardo & Niranjan, 2006). Even though making the same considerations for initial conditions that the previous models do, Cleland's Model estimates heat transfer based on empirical equations. This gives the advantage not only of Cleland's model to allow temperature variation, but also to consider that properties are not constant in the food. Freezing time can be estimated using the following equation:

$$t_{slab} = \frac{R}{h}\left[\frac{\Delta H_1}{\Delta T_1} + \frac{\Delta H_2}{\Delta T_2}\right]\left(1 + \frac{N_{Bi}}{2}\right) \quad (8)$$

This equation is valid for Biot numbers between 0.02 and 11, Stefan numbers between 0.11 and 0.36 and Plank numbers between 0.03 and 0.61. Table 1.2 contains the equations used to estimate ΔH_1 , $\Delta H_2, \Delta T_1, \Delta T_2$.

Table 1.2: Equations and variables involved in Cleland's model (Pardo & Niranjan, 2006)**.**

$\Delta H_1 = C_u\,(T_i - T_3)$	C_u: $unfrozen\ volumetric\ specific\ heat\ capacity\ \frac{J}{m^3K}$
$\Delta H_2 = H_L + C_f\,(T_3 - T_f)$	C_f: $frozen\ volumetric\ heat\ heat\ capacity\ \frac{J}{m^3K}$
$\Delta T_1 = \frac{(T_i + T_3)}{2} - T_a$	H_L: $latent\ heat\ of\ fusion\ \frac{kJ}{kg}$
$T_3 = 1.8 + 0.263\,T_f + 0.105\,T_a$	T_i: $initial\ temepature$
$\Delta T_2 = T_3 - T_a$	T_a: $chamber\ temperature$

1.4 Processing after freezing

Microstructural effects of freezing rate have been studied for almost 100 years. Nevertheless studies regarding processes after freezing are still in early stages. Nevertheless several fields have studied the effects of freezing on microstructure of different products containing wheat. Microstructural integrity has been shown to be affected by slow freezing treatments in sweet dough formulations (Meziani et al., 2012; Meziani et al., 2011). Slower freezing rates provided lower volume and gas expansion, as well as an increased rupture and reduced elasticity to dough, which was correlated to a damaged gluten structure. Viscoelastic and structural properties were also reviewed: the large ice crystals formed during slow freezing contribute to starch retrogradation and protein aggregation processes, which reduce elasticity and contribute to dehydration. Some studies regarding freezing of bread have been made. When the effect of the

freezing rate on dough was studied, it was shown that fast freezing rates produced a firmer bread (Malkki et al., 1974). Both studies suggest that microstructure can be affected even before the processing of foods, being the freezing of dough an important parameter in its properties. Carra et al. (2006) studied the effect of freezing in part-baked bread and concluded that the oral texture (crust crispness and crumb firmness) was enhanced compared to fresh bread, supporting the theory that freezing helps a more packed microstructure. (Gómez et al., 2011) found that freezing increased batter density and viscosity, and consequently decreased cake volume and height, but increased hardness. Baking after freezing has shown to be greatly affected by the freezing process, especially in surface properties as hardness, crispness or volume expansion. Considering this, surface properties should also be affected in a frying process, which would affect the oil absorption mechanics. Boiling after freezing of carrots was studied by Fuchigami et al. (1995), who noticed that quick-freezing resulted in better texture than slow-freezing, which was related to a higher deterioration of the structure due the loss of pectin, suggesting any food structure can be affected by freezing. Effects of freezing have been also studied on batter covered squid rings. Products that have been frozen have shown an increased absorption of oil which was explained by the deterioration that freezing caused to the squid substrate and the coating layer of batter; fissures produced by the growth of ice crystals probably favor the release of water and the penetration of frying oil (Llorca et al., 2001). In another study Llorca et al. (2007) reviewed the effects of freezing on the proteins of squid, revealing a shrinkage of the cellular structures (both of the batter and the squid) and the appearance of voids in the microstructure of the rings as a consequence of the packing of the protein fibers. Proteins are the main structural element in formulated snacks and packing of this element, due to freezing, would induce a more compact crust, making it harder for oil to penetrate into the structure.

Processing treatments after freezing may dehydrate the product, because of the loss of water involved in high temperature processing. There might be similarity between freeze-drying and the freeze-frying process, especially regarding the surface changes involved in both processes. The freeze drying process involves a fast freezing of

foods which helps preserving original properties, which could hold resemblance to a freeze-frying process. Some researchers have studied the effect of the freezing rate, thereby the effect of crystal size in freeze drying. Lee and Cheng (2006) studied the effect of freezing rate in nanocrystal dispersions and showed that different powder distributions could be formed. Drying of collagen scaffolds was studied by O'Brien et al. (2004), who demonstrated that a faster cooling rate produced more homogeneous ice crystals, which had a reduction in pore size. At a microstructural level it has been proven that freezing rate affects ice crystal distribution. Moreno and Bouchon (2008) studied the effect of freeze drying prior to frying on potato chips. The process increased oil suction compared to the control, mainly because of the external porous structure that reduces the resistance to oil absorption. There was a fast freezing of potatoes before they were processed, which preserved the structure and thereby increased oil absorption. The effect of freezing rate on soursop fruit pulp was studied by Ceballos et al. (2012). Faster freezing increased wettability time of freeze dried soursop powders as a result of the reduction in ice crystal size, mean pore diameter and the resultant increment in capillary tortuosity. Freezing rate of acerola fruit was studied by Marques et al. (2007).They found that faster freezing rates preserved the original porous structure the best. If fast freezing and post frying holds resemblance with freeze-drying it is probable that results will be similar, that is, a better preservation of the porous structure, which in the case of frying should increase oil penetration.

2 HYPOTHESIS

As it has been exposed, no relationship has yet been established between the freezing and the post frying processes of formulated products. Different rates of freezing produce different sizes and distribution of water crystals. In formulated products this is especially important, because of its structural components, particularly gluten. If the gluten network gets affected, the whole microstructure and transport phenomena related to frying will be affected.

Accordingly, the hypothesis of this thesis states that the rate of freezing affects the microstructure of raw dough and therefore the developed microstructure during deep-fat frying and the associated oil absorption capacity of the matrix.

Specifically, it is believed that two different rates of freezing will produce different products, even when using the same formulation and frying conditions. Also, it is expected that a fast freezing rate will produce smaller and homogeneous crystals, which will preserve the microstructure of the matrix. On the other hand, it is believed that large and less homogeneous crystals will be produced during slow freezing, which will produce a less firm and strong microstructure after frying. These changes should be observed in the microstructure of the food matrix and in the transport phenomena related to frying (moisture loss and oil absorption).

3 OBJECTIVES

In concordance, the objective of this thesis is to understand the effect of the freezing rate on the microstructure of gluten and starch formulated dough during deep-fat frying and associated transport phenomena, particularly oil absorption.

The specific objectives are:

1) To develop a reproducible procedure that allows the characterization of the freezing process of formulated dough,

2) To understand the relationship between microstructure development and transport phenomena after freezing at two different rates (fast and slow),

3) To give an integrated vision of the freezing and frying processes, which have been only analyzed individually until now.

4 MATERIALS AND METHODS

4.1 Materials

Products were formulated using a reconstituted blend of wheat gluten (Asitec, Chile) and wheat starch (Molinos Juan Semino, Argentina), instead of wheat flour, to accurately control ingredients proportion. High oleic sunflower oil (Camilo Ferrón, Chile) was used as frying medium.

4.2 Product formulation

Dough was prepared ensuring 10% gluten (d.b.), 90% starch (d.b.) and a water content of 70% (d.b.). The amount of water added depended on the initial water content of the ingredients and was adjusted to ensure that all different products contained the specific amount. To determine the amount of water that had to be added, the exact water content was determined experimentally by drying in a forced-air oven (LDO-080F, Labtech Korea) at 105°C to constant mass.

4.3 Sample preparation

Products were prepared by mixing the dry ingredients for 2 min using a 5K5SS food mixer (KitchenAid, USA), equiped with a 5KAB flat beater. To form the dough, distilled water was added according to the protocol described by (Gazmuri & Bouchon, 2009). Half of the water was gradually added at 15°C while mixing for 1 min. After mixing for 1 extra min, the remaining water was added. This fraction was heated at 90°C, and was also poured while mixing for 1 min. The blend was then mixed for 1 min. The dough was then wrapped in a plastic bag for 1 h at room temperature (20°C). After dough formation, it was kneaded to ensure homogeneity, laminated to the required thickness using a dough sheeter (DOYON-LSB516, Canada), and cut into 10cm diameter cylinders. Two different thicknesses were sheeted, 10mm (thick discs) and 5mm (thin discs), aiming for an infinite lab geometry. Discs were weighted to ensure the same solid contents for each sample.

4.4 Freezing

Table 4.1: Frying and freezing times (min) of different discs and different moisture contents.

	S-Thick	F-Thick	S-Thin	F-Thin
Freezing	54	21	34	14
30% W	14	13	7	6,5
40% W	11	10	5,5	5
50% W	9	8	4	3,5

Discs were frozen at two different rates until the center reached -18°C. Fast freezing was carried in an air blast freezer (Irinox M.LC 51/25, Italy), using the shock freezing program, whereas slow freezing was carried in a conventional freezer at -18^{o}C (General Electric, GTS16DTHWW, Chile). Freezing was ended when the center of the disc achieved -18°C. Freezing times for fast-frozen thick discs (F-Thick), slow-frozen thick discs, fast-frozen thin discs (F-Thin) and slow-frozen thin discs (S-Thin) are shown in Table 4.1. Afterwards, frozen thick and thin discs were conditioned prior to frying, during 2 and 1 min, respectively.

4.5 Frying

Frozen discs were fried at 170±2°C in a 5-L capacity deep-fat fryer (Somela-535T, Chile), equipped with an external temperature control system (PID + Autotuning, Veto, Chile), until reaching final moisture contents of 30, 40 and 50% (d.b.). Frying times of the different samples are presented in Table 4.1. The fryer was filled with 4 L of oil that was preheated for 2 h prior to frying (Blumenthal, 1991) and was discarded after 180 min of frying time. Throughout the frying process, frozen discs were placed in a basket and held in position with a wire grid to prevent them from floating. When frying was completed, the products were removed from the fryer, and the post-frying cooling period began.

4.6 Temperature measurement

In order to record temperature variations throughout the freezing-frying process, 0.5-mm diameter K thermocouples (Veto, Santiago, Chile) were inserted at different heights within the discs. In thin discs the center and the surface temperatures were measured, whereas in thick discs, the temperatures at 1.5 and 3 mm from the center were also measured. To ensure that thermocouples were inserted in the same position in all experiments (see Figure 4.1) a metal structure was designed, which surrounded the disc and had holes at the different heights, allowing a reliable insertion of thermocouples. All, but the surface thermocouple, were inserted along the axis up to the center of the disc. The surface thermocouple was inserted through a diagonal hole on the metal structure, as depicted in the Figure, up to the surface. Data were collected every 10 s using a data logger (Visual Hotmux 3.1.0, Veto, Chile). The measurements were carried out in triplicate for each of each product category (F-Thick, S-Thick, F-Thin and S-Thin).

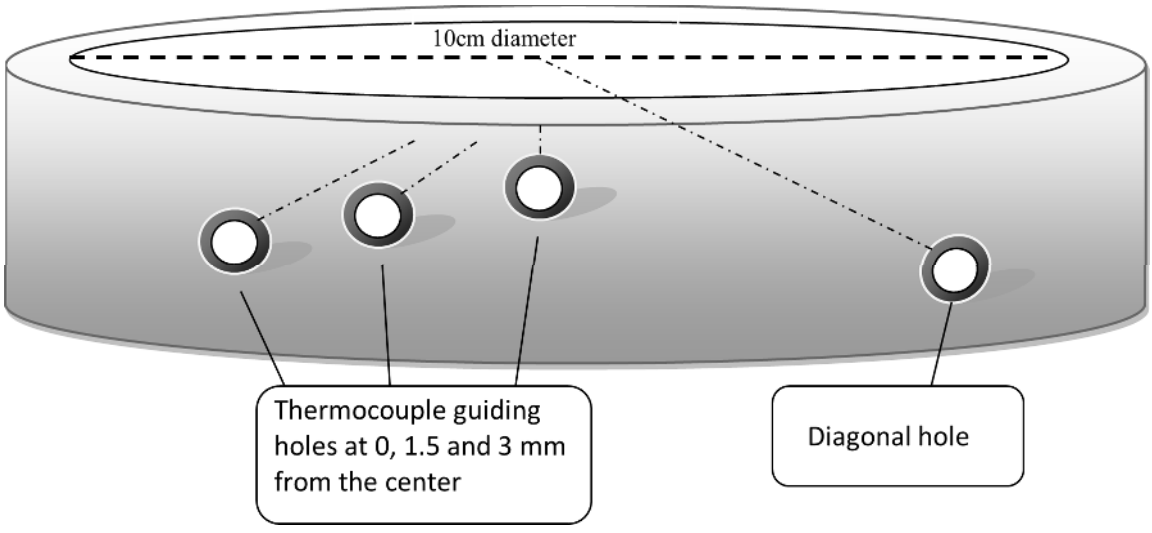

Figure 4.1: Diagram of the metal structure used to ensure a controlled location of the thermocouples within the dough.

4.7 Analytical methods

Two different oil fractions were determined, *surface oil,* which was defined by Bouchon et al. (2003) as the amount of oil that is easily removed and therefore just remains on the surface of the product and *penetrated oil,* which considered the total amount of oil after surface oil removal. That is, it corresponded to the addition of penetrated surface oil and structural oil fractions, as coined by Bouchon et al. (2003).

Surface oil (SO) was determined gravimetrically after immersing each sample during 2 s in 800 mL of petroleum-ether (Heyn, Chile) at room temperature, by weighing the remaining oil after solvent evaporation under vacuum. Surface oil was removed at equilibrium, after 10 min of cooling, allowing drainage at room temperature (20°C). Samples were hold in a vertical position, so that excessive surface oil could drain off. The resulting solution was transferred several times to a 250 mL round bottom flask (Quickfit-BDH, Poole, UK) that had been previously dried and weighed. Finally the extracted oil was collected by evaporating the solvent under vacuum (0.7 bar) using a rotatory evaporator (BÜCHI Rotavapor R-124, Switzerland). The flasks containing the extracted oil were then dried to constant mass, by heating in a convective hot air oven at 105°C, cooled in a desiccator and weighted (Bouchon et al., 2003).

Penetrated oil content (PO) was determined after SO removal. The samples were ground and dried in a forced-air oven at 105°C for 24 hours (to less than 10% moisture content). Then samples were transferred into cellulose paper extraction bags. A clean, dry round bottom flask (250 mL) was weighed and 200 mL of petroleum-ether were added to the flask. Extraction was carried out for 4 h using a soxhlet apparatus (70°C) and the solvent was removed using a rotatory evaporator. The flasks containing the extracted oil were then dried to constant mass, cooled in a desiccator and weighted (AOAC, 1995; Bouchon et al., 2003).

Total oil content (TO) was determined as the sum of SO and PO. Fat content of the samples prior to frying was neglected.

Solids content was determined by drying the defatted samples, using a forced-air oven at 105°C for 24 h until a constant mass was reached (AOAC, 1995).

Moisture content (W) of the samples was determined before and after frying on each experiment to determine moisture loss. This was carried out by air drying 3 g of ground sample at 105°C until constant mass was reached (AOAC, 1995).

To test for reproducibility four batches were prepared, sheeted, frozen and fried for each formulation. Also four batches were prepared for temperature measurements.

4.8 Microstructural analysis: Confocal laser scanning microscopy

Microstructural analyses were carried out to examine the extent of oil penetration and its distribution inside the fried discs. Non-invasive observations were attempted using confocal laser scanning microscopy (CLSM). For this purpose frying oil was coloured with a fluorescent dye. Nile Red (Sigma Aldrich, Germany) was used as the oil marker as it has been found to be a suitable heat resistant and lipid soluble fluorochrome. A concentration of 0.05 g of Nile red per litre of oil has been found to give a good emission (Pedreschi et al., 1999).

4.8.1 Sample preparation

The analysis was centered on products with 40% moisture (d.b.), as a base case, since they are ideal to process in comparison to other products which are either too crumbly (30% moisture d.b.) or too soft (50% moisture d.b.). Two samples of each product category were prepared and from every sample two sections were extracted, obtaining 4 replicas for each condition. Small sections of 1 mm^2 were cut manually from every sample using a N° 10 scapel blade (Diatome, PA, USA). The section was then fixed to a 20x20mm^2 glass cover slip (Meisterglass ®) in order to preserve the crust. Cross section was observed under the microscope as showed in Figure 4.2.

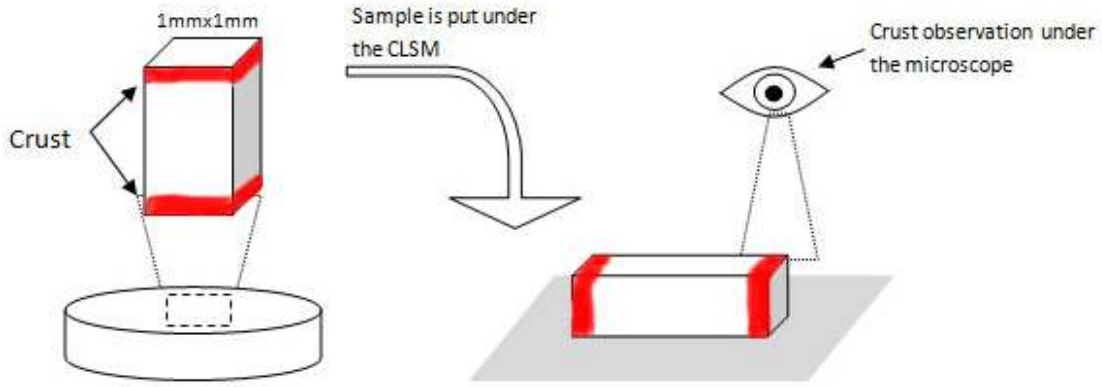

Figure 4.2: Schematic diagram of the cut and observation process used for the microscopical observations. Figure on the left shows how the cut is extracted from the disc and figure on the right shows the same cut under the microscope.

4.8.2 Preliminary observations

Preliminary observations were arried out using epifluorescence microscopy (EFM) in a Olympus SZ2-ILST microscope (Arquimed, Santiago, Chile) equipped with a CoolSnap Pro cf. Color camera (Arquimed, Santiago, Chile). The excitation range used was 545-580nm. Separated panoramic pictures of the cross section were taken, using fluorescence and reflected light. Then images were merged into one single image using Photoshop CS5, to get the complete cross section.

4.8.3 Final experiments

Inner microstructure was observed in an IX81 motorized inverted CSLM (FluoView1000, Olympus, Japan) in its fluorescent mode. The Nile-red-stained oil was observed after exciting at 543 nm with the Helium/Neon laser. Emissions were collected over 560 nm. Digital image files were acquired using a 10x magnification objective lens (0.3NA) over regions of 1024x1024 pixels^2 with a resolution of 0.787 μm/pixel in x and y directions. Image acquisition was performed with a pinhole size of 90 μm when collecting the Nile red emission. Focal plane was obtained at a depth of 200 μm from the

surface in order to minimize cut effects. Four images were acquired and averaged to obtain every final image.

4.8.4 Image processing and analysis

ImageJ (Rasband, W.S., U. S. National Institutes of Health, Marylandd) was used for image processing. In order to estimate the thickness of the oil layer the following procedure was used:

i) Threshold using Otsu method was applied to images in order to ensure first point of detection was actually crust, avoiding effects of noise (image on middle Figure 4.3).

ii) A tangent line to the outer crust was traced, which began where fluorescence was first detected (yellow line on the left hand side of Figure 4.3).

iii) The tangent line was then transported towards the core, until no more fluorescence was detected (yellow line on the right hand side of Figure 4.3).

iv) The distance between both lines was measured and considered as the crust thickness. (green line).

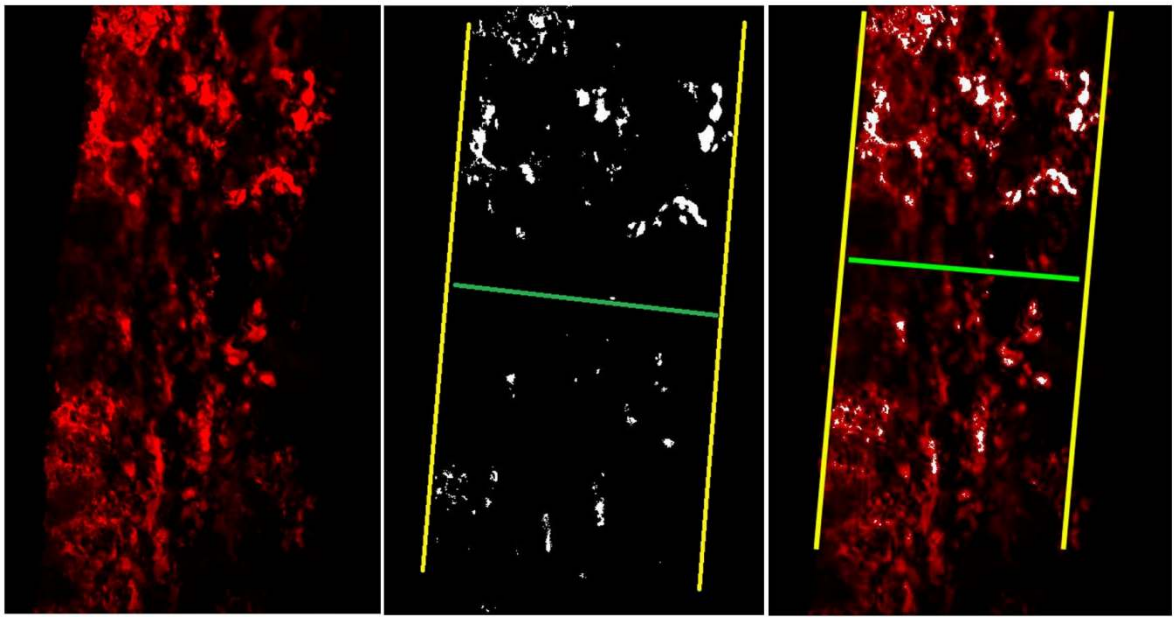

Figure 4.3: Schematic diagram of image processing for crust thickness estimation. On the left the original image is presented. Middle image is the resultant of the otsu threshold, presented with schematic lines that explain the process to establish thickness. On the right the superposition of the first to images is shown.

Analysis was carried under no further processing of images, even though in some images presented in the results, contrast is enhanced in order to make results more clear.

5 RESULTS AND DISCUSSIONS

In the next sections, results about temperature profiles during freezing and frying are analyzed, which are used to understand oil absorption kinetics and associated microstructural changes.

5.1 Temperature Profiles

The temperature profiles during freezing and frying of the four different products are shown in Figures 5.1 to 5.4. In every figure the critical times of the process are presented: the end of freezing, the beginning of frying as well as the frying times that were needed to achieve 30, 40 or 50% (d.b.) moisture content.

It can be seen that the freezing process started at room temperature, which is about 20°C. Then it descended linearly until reaching 0°C, a period of time that was defined as the initial cooling period, as shown in Table 5.1. This period lasted 13 min in S-Thick discs, and was reduced in approximately 40% during fast freezing (F-Thick discs). In thin products, differences during initial cooling were not so marked, diminishing from 6 to 5 min, in S-Thin and F-Thin products, respectively.

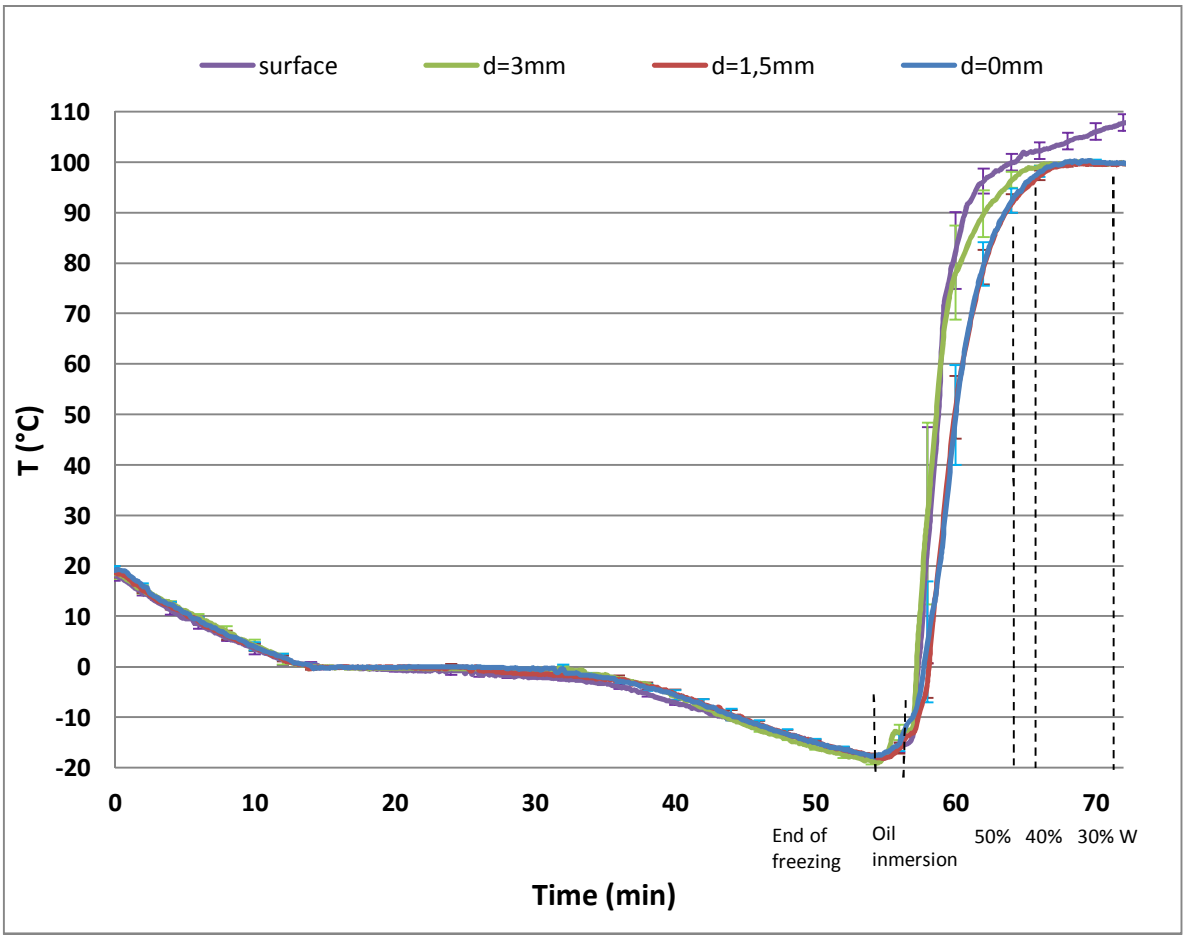

Figure 5.1: Temperature profiles in different locations during slow freezing and frying of thick discs, showing the end of freezing, the beginning of deep-fat frying and the frying times needed to achieve 30, 40 or 50% (d.b.) moisture content (mean values ± standard deviation, n=3).

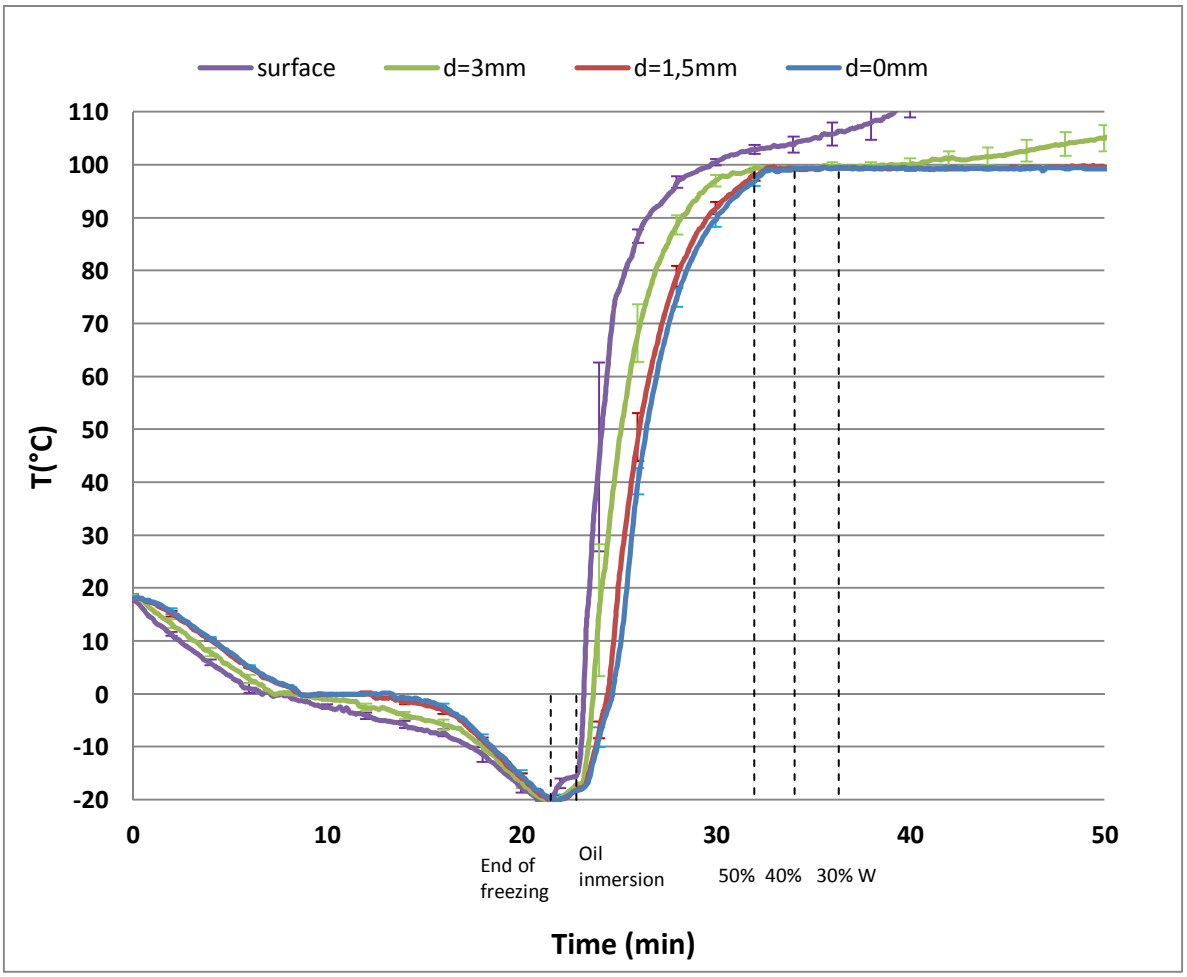

Figure 5.2: Temperature profiles in different locations during fast freezing and frying of thick discs, showing the end of freezing, the beginning of deep'fat frying and the frying needed to achieve 30, 40 or 50% (d.b.) moisture content (mean values ± standard deviation, n=3).

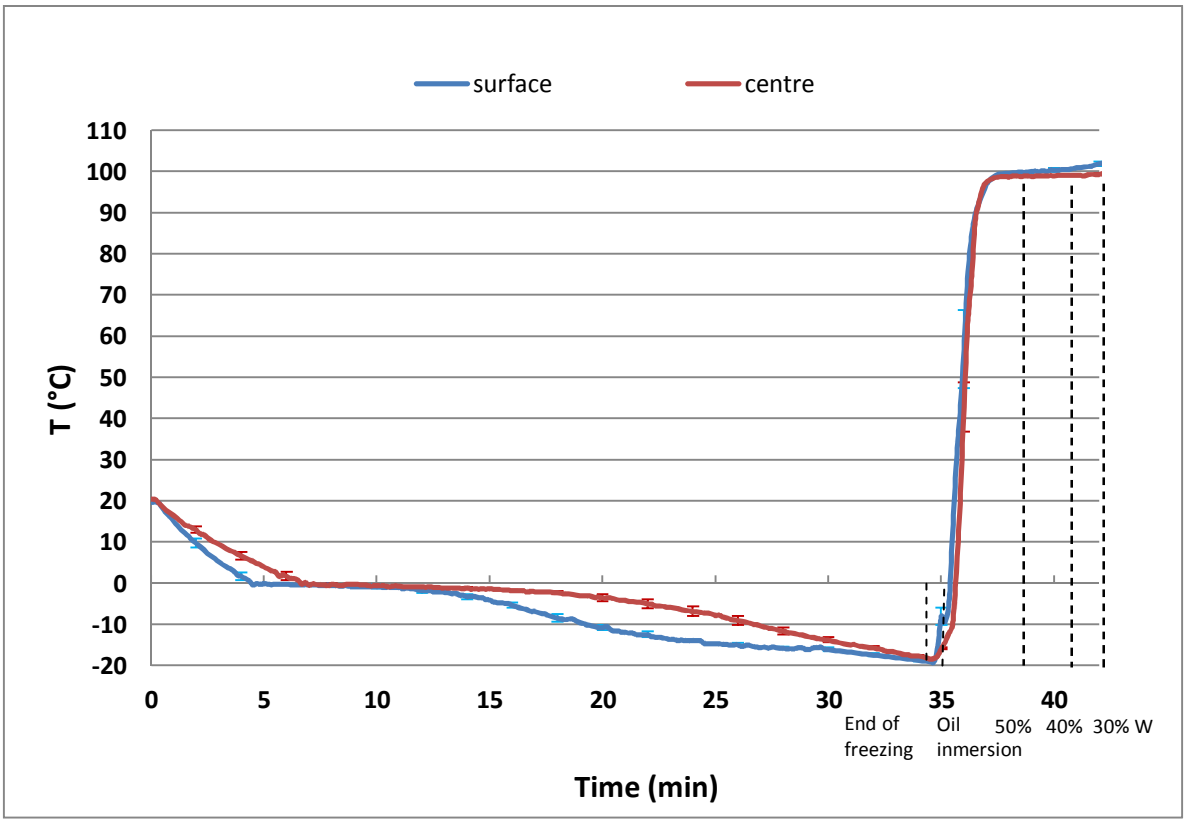

Figure 5.3: Temperature profiles in different locations during slow freezing and frying of thin discs, showing the end of freezing, the beginning of deep-fat frying and the frying time needed to achieve 30, 40 or 50% (d.b.) moisture content (mean values ± standard deviation, n=3).

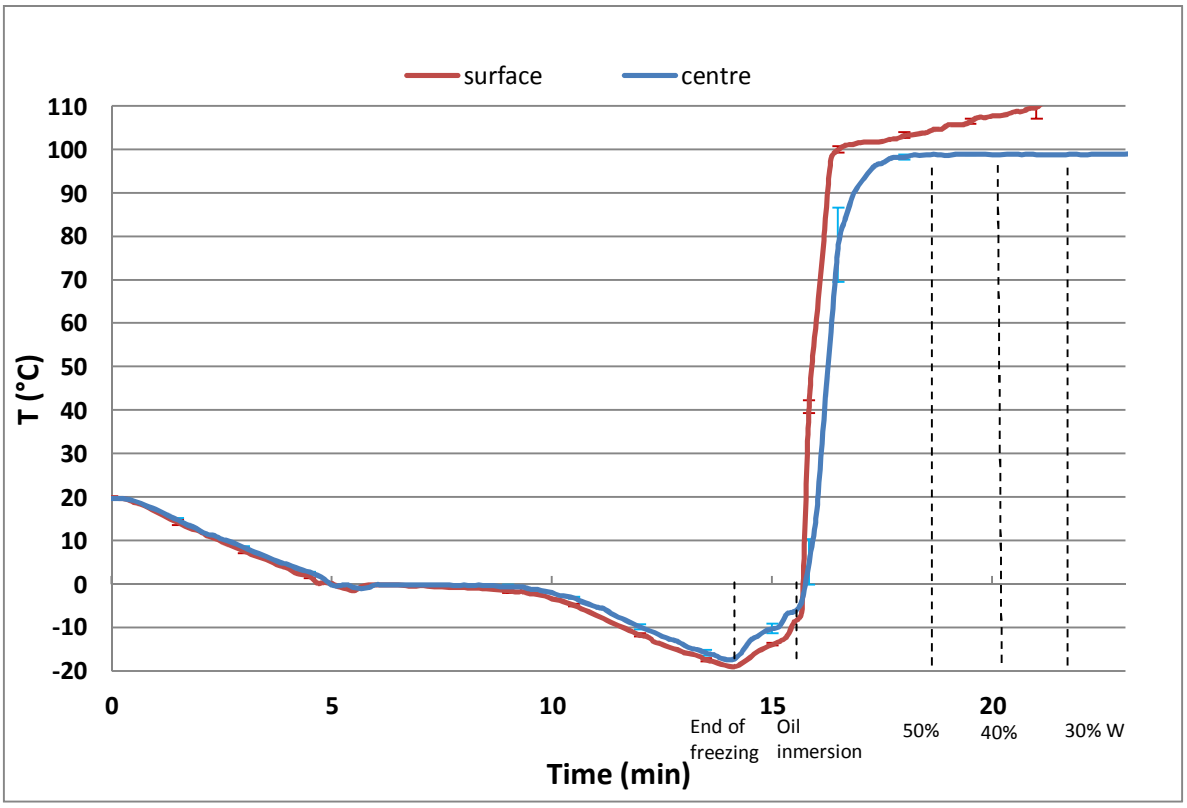

Figure 5.4: Temperature profiles in different locations during fast freezing and frying of thin discs, showing the end of freezing, the beginning of deep-fat frying and the frying time needed to achieve 30, 40 or 50% (d.b.) moisture content (mean values ± standard deviation, n=3).

After the initial cooling period the temperature profile of the thermocouple placed at the center of each product (d=0mm) reached a plateau during different periods of time as shown in Table 5.1. If can be seen that the period of time that the sample remained at the freezing plateau increased significantly when the freezing process was slowed down. In thick products this period of time increased in 240%, whereas in thin product an increased in 50% was determined. This suggests that larger crystals should be formed during slow freezing. During this period of time the dissolved solids should concentrate and a great fraction of the liquid water should freeze. This is a critical

period, about 73% of the water should crystalize during this time interval (Plank, 1963). The remaining unfrozen water would freeze as cooling progresses.

Table 5.1: Freezing times of different samples separated into initial cooling, freezing plateau and final cooling periods. Freezing rate was calculated as the ratio between the semi thickness and the time needed to achieve -18°C (from 0°C) at the center of the product.

	S-Thick	F-Thick	S-Thin	F-Thin
Initial Cooling (min)	13	8	6	5
Freezing Plateau (min)	17	5	6	4
Final Cooling (min)	24	8	22	5
Total Time	54	21	34	14
Freezing Rate (cm/h)	0,73	2,31	0,53	1,67

The freezing process continued until the temperature of the core reached -18°C. In the case of slow freezing, which was carried out in a normal freezer, the surface temperature could not go below -18°C. In the case of fast freezing, the environment temperature was at -30°C. Thus, the surface temperature was slightly below -18°C (approximately -20°C), when the center reached the final temperature. Overall, the whole freezing process was 2.57 and 2.42 times longer in slow freezing compared to fast freezing, when freezing thick and thin products, respectively. As it was mentioned in the introduction section, some authors have defined the freezing rate as the quotient of the thickness of the frozen region divided by the time needed to freeze it, from 0°C. Results of the different freezing rates, taking into account this approach, are presented in Table 5.1, which clearly shows important differences between slow and fast freezing. These

results agree with those reported by Plank (1963), Rahman (2007) and Sun (2011), who defined that fast freezing requeires a minimum freezing rate of 1.5 cm/h.

Certainly, frying is a much faster process than freezing. When frozen discs were immersed in the oil bath, the temperature rose extremely fast. Subsequently, the temperature rise of the outer layers slowed-down when approaching to the boiling point of water and speed-up once again, when the water present in that portion evaporated. This is a direct consequence of frying, which is characterized by a water-evaporation moving front that defines a crust region that may exceed the boiling point of water (no liquid-water is left) and a core region, which is limited to the boiling-point of the interstitial liquid, which may be slightly higher than the boiling point of water due to the presence of solutes (Bouchon, 2001). This can be clearly seen in Figures 5.1, 5.2, 5.3 and 5.4, where the core region is limited to approximately 100^{o}C. Intermediate layers of the structure could or could not rise above 100°C, depending of the freezing process, as will be later discussed.

Differences between samples can be better observed in Figures 5.5 and 5.6, which show the surface temperature increase in the surface and the center regions, respectively. In fact, longer times were needed to reach the same moisture content in slow-frozen products compared to fast-frozen ones. This is probably because bigger crystals were formed during slow freezing, which are harder to melt (Plank, 1963; Rahman, 2007). The same effect was seen in other systems, such as ice cream, where bigger ice crystals were harder to melt (Muse & Hartel, 2004) and aqueous polymer solutions , where matrices with bigger crystals were more difficult to freeze-dry, increasing sublimation time (Kochs et al., 1991).

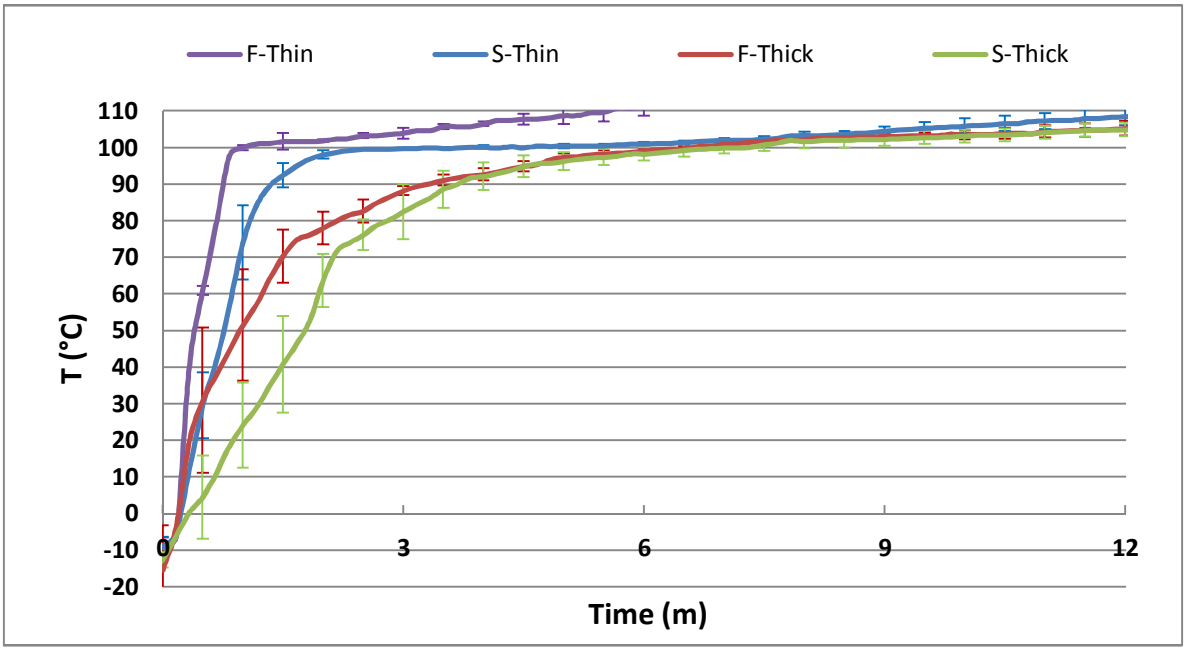

Figure 5.5: Temperature profiles on surface during frying of thick and thin discs frozen at fast and slow freezing rates (mean values ± standard deviation, n=3).

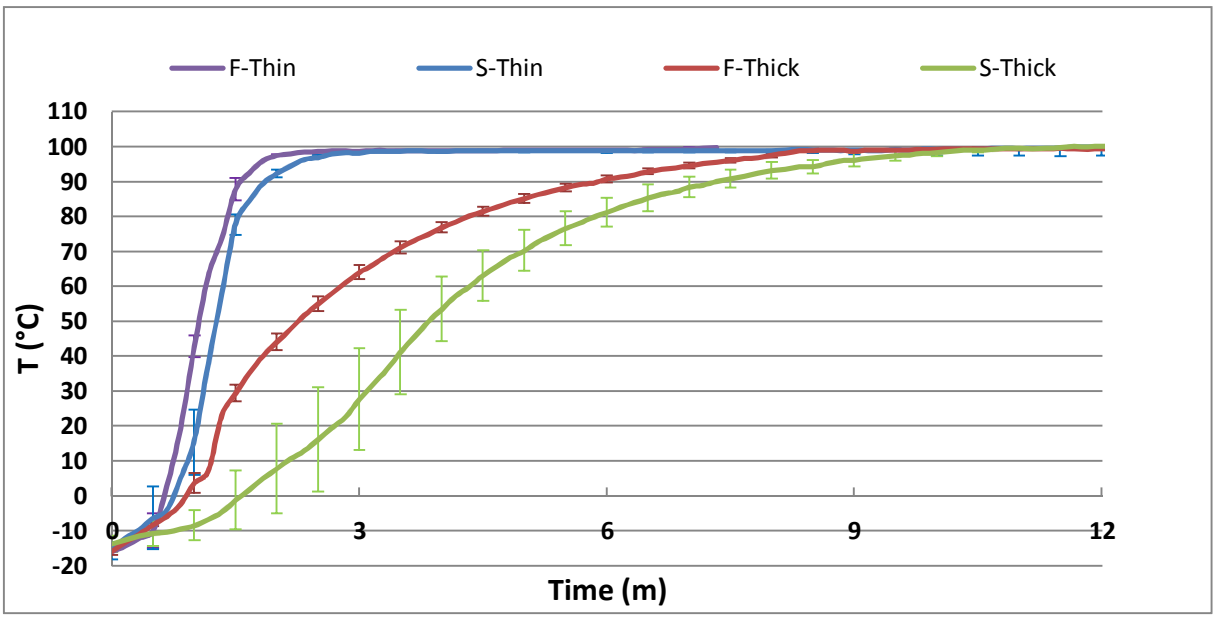

Figure 5.6: Temperature profiles on centre during frying of thick and thin discs frozen at fast and slow freezing rates (mean values ± standard deviation, n=3).

Faster heating not only means faster crystal melting, but also faster crust formation. This is reflected in Figure 5.7, which shows the temperature increase in thick products at 3 mm from the center (i.e. at 2 mm below the surface). It can be seen that after approximately 15 min the moving front moved further towards the interior in fast-frozen products, since the temperature exceeded 100°C at this location, denoting faster crust formation. It is important to note that in fast-frozen products microstructure is possibly better preserved than in slow-frozen ones, since melting of large ice crystals, may induce inner structure collapse and packing, decreasing oil permeability. On the other hand fast freezing may better preserve food microstructure, as it was shown upon frying freeze-dried samples (Moreno & Bouchon, 2008).

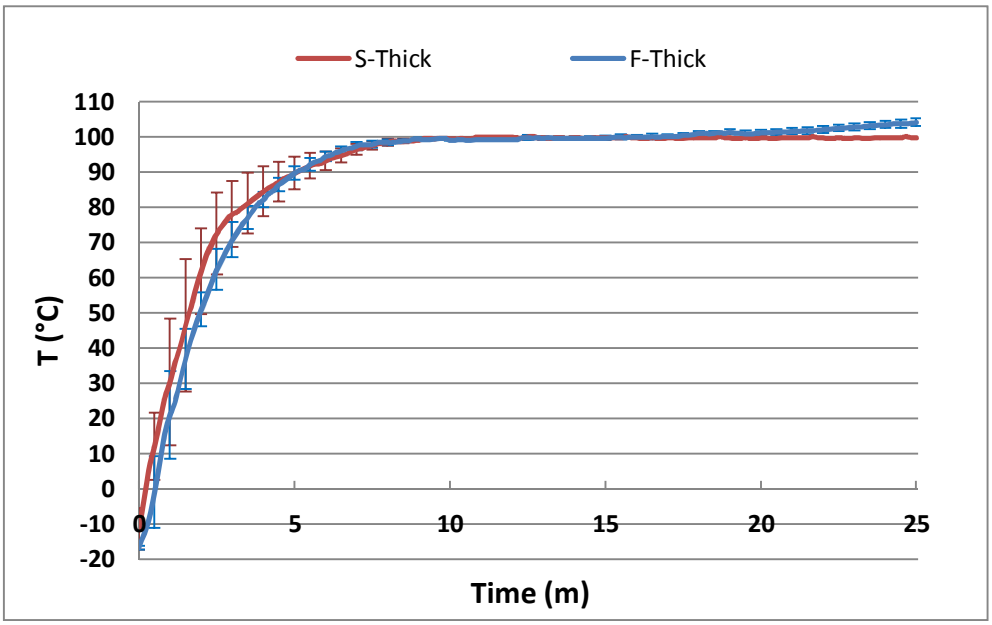

Figure 5.7: Temperature profiles at 3mm from the centre during frying of thick discs frozen at fast and slow freezing rates (mean values ± standard deviation, n=3).

5.2 Oil absorption

Oil content of the different samples was determined in order to understand its relationship to slow and fast freezing. To do so, penetrated oil (PO) and surface oil (SO) fractions were determined, as explained in section 4.7.

5.2.1 Total oil content

The total oil content of the four different product categories, which were fried up to different moisture levels (50%, 40% and 30% d.b.) are presented in Figure 5.8. Overall, it can be observed that all products increased their oil intake when the dehydration was increased (30% d.b. final moisture). These results are consistent with those previously reported in other systems (Bouchon et al., 2003; Gazmuri & Bouchon, 2009; Moreno & Bouchon, 2008). As was explained before, oil suction takes placed mainly after the disc is removed from the oil bath. Thus, up to a certain extent it corresponds to a water replacement phenomenon. Oil takes place where water was previously located, making total oil content highly dependent on the final moisture content of the product, thereby on the frying time.

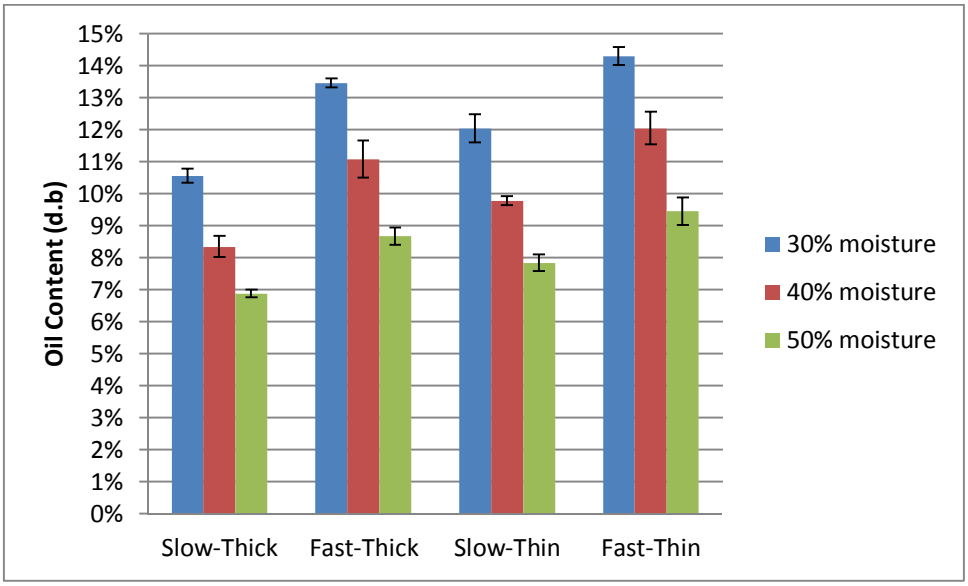

Figure 5.8: Total oil content of samples fried until moisture contents of 50, 40 and 30% d.b.(mean values ± standard deviation, n=4).

The relationship between moisture loss (from an initial moisture of 70% d.b.) and oil uptake, for each product category, can be clearly seen in Figure 5.9. A good linear correlation can be observed for each product category. However, an overall correlation cannot be established, since different product categories absorbed different amounts of oil for a given moisture loss. Certainly other factors, such as porosity, may affect this behavior (Dueik and Bouchon, 2011).

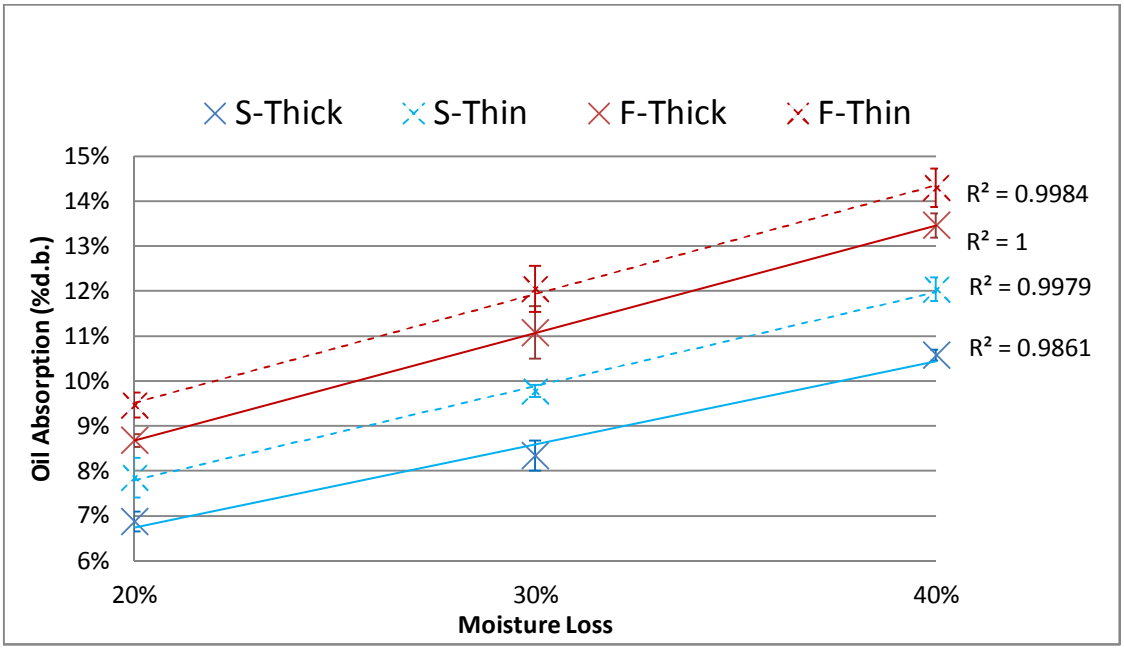

Figure 5.9: Relationship between moisture loss and total oil absorption in different products (mean values ± standard deviation, n=4).

With respect to the effect of freezing on oil absorption, it can be clearly observed that slow freezing decreased significantly ($p<0.05$) oil-uptake during deep-fat frying. This may be due to the formation of large ice crystals, which may induce inner structure collapse during melting, decreasing permeability to oil. In other fields, freezing rate has shown to affect microstructure of foods. In freeze-thawing cycles, Carbonell et al. (2006) confirmed better potato tissue integrity retention with faster freezing rates.

Ceballos et al. (2012) showed that faster freezing rates affected the wetting time because they produced decreasing pore size and increased tortuosity on freeze dried soursop fruit pulp. A better retention of the original shape and volume of the food product may favor oil flow within the structure, increasing oil absorption, as reported by Moreno and Bouchon (2010), after frying freeze dried samples. On the other hand, (Meziani et al., 2011) found that low freezing rates resulted in elasticity reduction, due to the dehydration of the dough network and starch retrogradation, as well as an increase of protein aggregation. These factors may well induce a structure collapse that may preclude the oil flow within it.

In order to better understand this phenomenon, the total oil content was divided in two fractions: one that remains on the surface and may be easily removed (surface oil, SO) and another one that is able to penetrate within the structure of the crust during the frying process, but mostly during the post-frying cooling period (penetrated oil, PO). At the end of the process, when the food is removed from the oil bath, there is a competition between drainage and suction, which defines the relative amount of these two fractions and consequently total oil absorption. Certainly, the final equilibrium is highly dependent on food microstructure.

5.2.2 Penetrated oil

Figure 5.10 shows penetrated oil fractions for the four different product categories, after frying up to the different moisture levels (50%, 40% and 30% d.b.). Overall, it can be observed that this oil fraction represents most of the oil absorbed by each product (varying from 79,7 to 94,5% of total oil content) and thus, it followed a similar patter to the one described in Figure 5.8

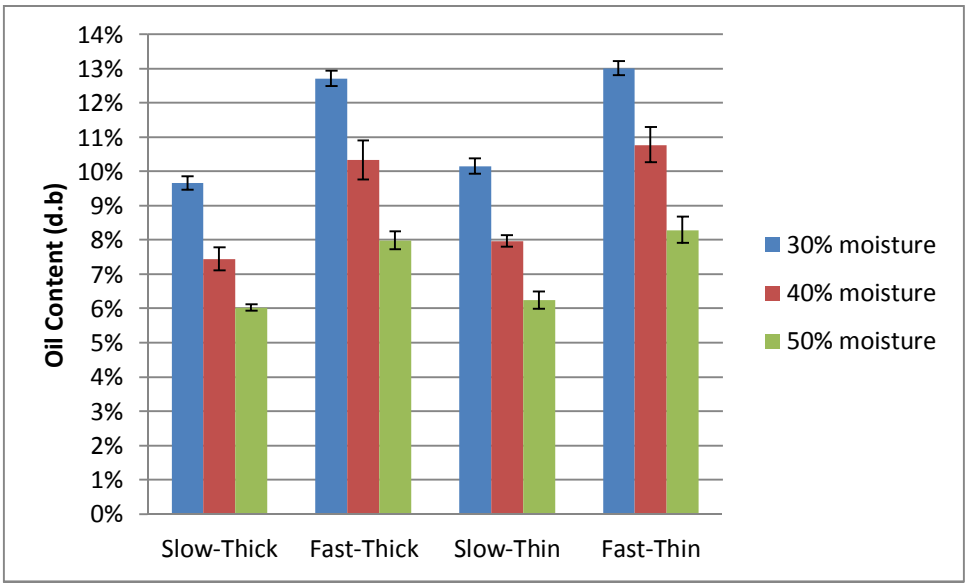

Figure 5.10: Penetrated-oil content of samples fried until moisture contents of 50, 40 and 30% d.b. (mean values ± standard deviation, n=4).

In fact, a good linear relationship between penetrated oil and moisture loss was determined, as can be seen in Figure 5.11.

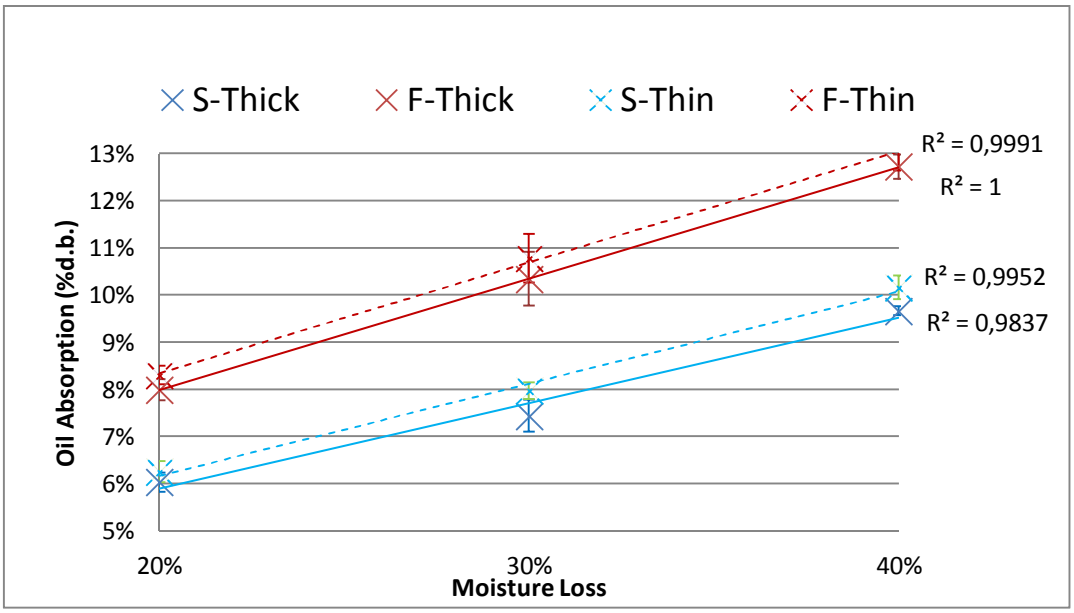

Figure 5.11: Relationship between moisture loss and penetrated-oil in different products (mean values ± standard deviation, n=4).

Penetrated oil is highly dependent on the moisture content, even more than total oil is. This happens because penetrated oil can only go into the structure if water evaporates, leaving an adequate space for oil infiltration (pores). Penetrated oil was also higher in fast frozen products ($p<0.05$), compared to slow frozen ones, probably due to the microstructure related explained before.

No significant differences ($p<0.05$) in oil absorption between thick and thin products were found, when analyzing the same moisture loss. Thus, the amount of oil that penetrated within the structure increased proportionally with the thickness, maintaining the oil/solids relationship. Due to the higher frying time needed to achieve the same moisture loss in thick products, a larger crust is formed, which maintains the oil/solids relationship for the different thicknesses. This confirms that oil penetration is a surface-related phenomenon, confined to the crust region, which is highly related to ice crystal formation and water loss.

Oil suction mainly takes place in the cooling period. There is a competition between drainage (which contributes to SO) and suction (which contributes to PO). For increasing frying time, due to larger crust formation, penetrated oil may increase, decreasing surface oil content. An inverse relationship during frying of potatoes between this two fractions has been shown, with a total overall increase in oil uptake due to further structure development for increasing frying times (Bouchon et al., 2003).

5.2.3 Surface-oil Content

Figure 5.12 shows the surface oil content for the four different product categories, after frying up to the different moisture levels (50%, 40% and 30% d.b.).

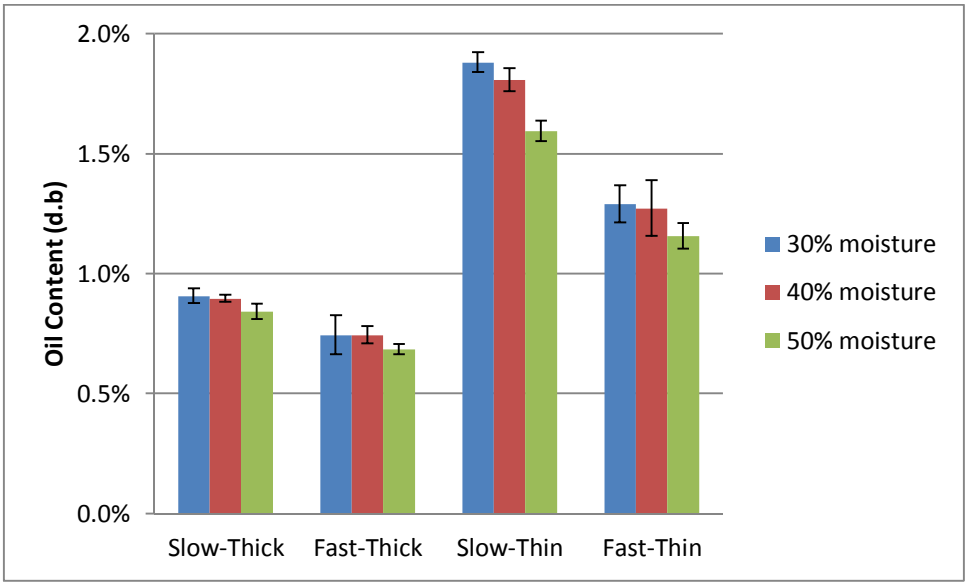

Figure 5.12: Surface Oil content of samples fried until moisture contents of 50, 40 and 30% d.b. (mean values ± standard deviation, n=4).

It can be seen that this fraction remained relatively unchanged for increasing frying times (higher moisture loss). No significant differences ($p<0.05$) in SO were observed for each product category, except from the s-thin product that showed a significant lower amount for the lower dehydration. Overall, differences in total oil absorption between thin and thick products are due to this oil fraction. These differences could be maybe

attributed to differences in surface roughness, which may reduce oil drainage in thin samples (Moreno et al., 2010).

5.3 Microstructural Analysis

In order to have a deeper understanding of the oil penetration phenomena, microscopical analyses were made to understand the relationship between crust formation and oil penetration distance. Products were directly fried in an oil bath that was previously died with Nile Red, a lipid-soluble and heat stable fluorochrome to be later observed under a confocal laser scanning microscope (CLSM). The 40% moisture products were observed, results which are shown below. In the case of thin products the whole section is presented. For thick products, which exhibited a double oil layer, selections of each layer were chosen.

A first point that must be noticed is that thick products presented a double layer of oil, which could be a consequence of the longer frying times that were needed, which may cause crust separation. The crust was divided into two layers that were separated by a void space; a good example is shown in Figure 5.13 (see Appendix D for original images). Analysis was focused on individual oil layers, consequently they were processed to show only one of the two oil layers. On the other hand, thin products presented a single layer of oil.

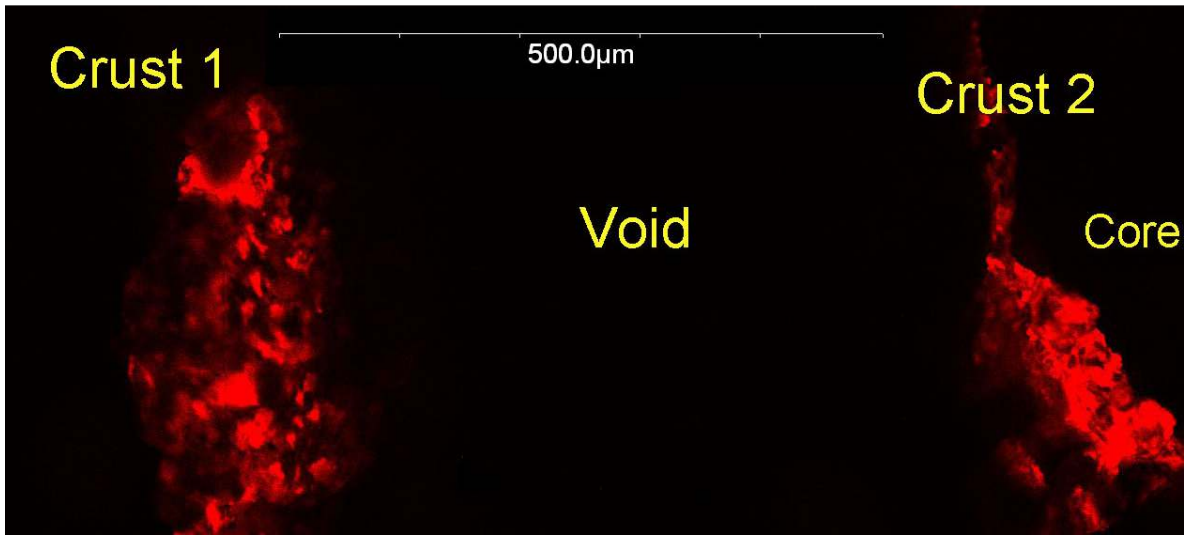

Figure 5.13: Example of double oil layer in thick products.

Figures 5.14 to 5.19 present the four different sets of images taken by CLSM for each product category. In the case of thick products both layers of oil are shown separately. In all sets of images the crust starts at the left hand side of the image and continues towards the core, at the right hand side. As a general observation it could be said that first oil layers usually look like a defined strip of oil, meanwhile the second layer has a more random shape. Even more defined shapes can be observed on thin products, where the line where the crust starts can be seen very clear in comparison to thick products.

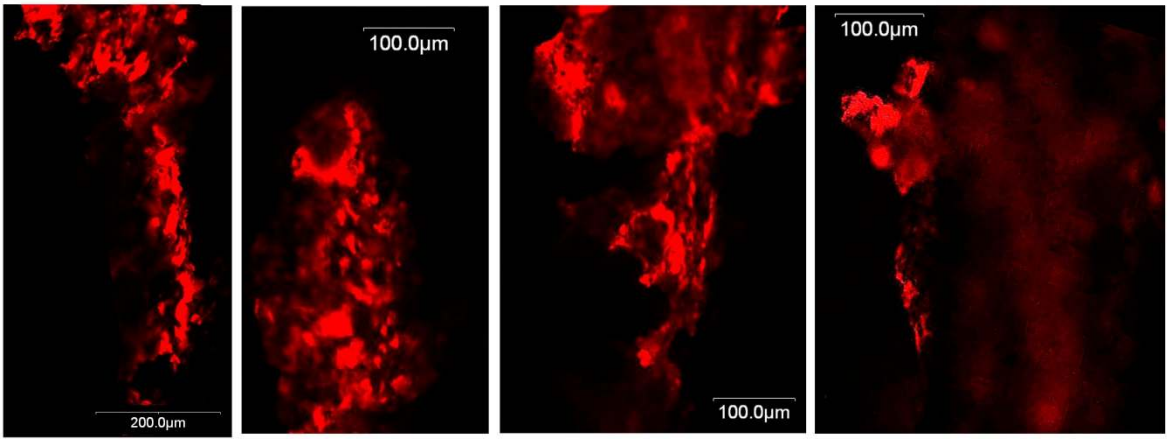

Figure 5.14: CLSM images of S-Thick samples: first oil layer

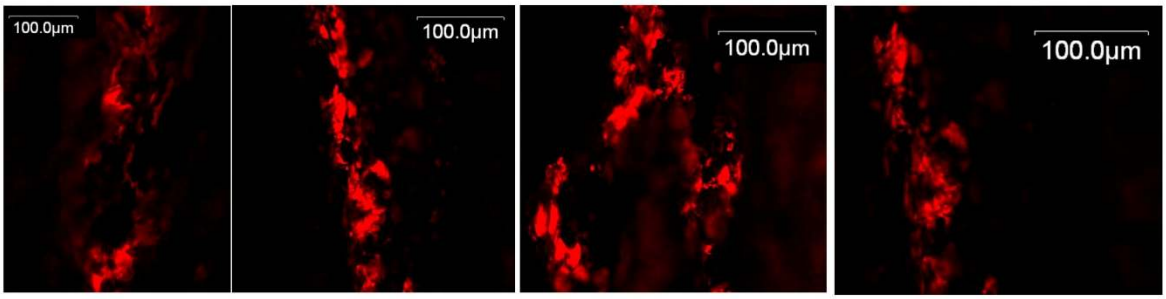

Figure 5.15: CLSM images of F-Thick samples: first layer of oil

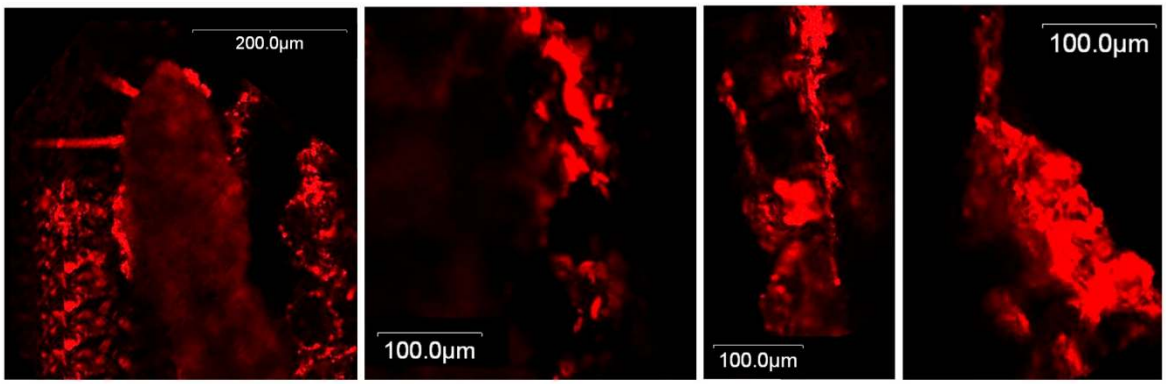

Figure 5.16: CLSM images of S-Thick images: second oil layer

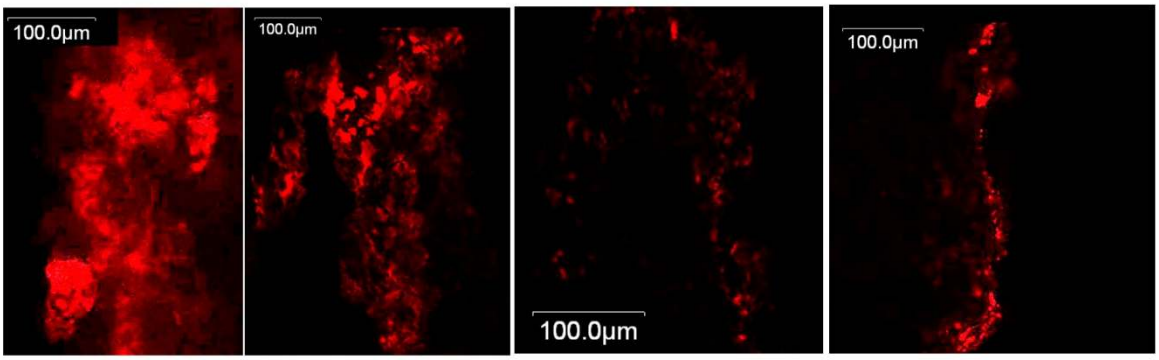

Figure 5.17: CLSM images of F-Thick images: second oil layer

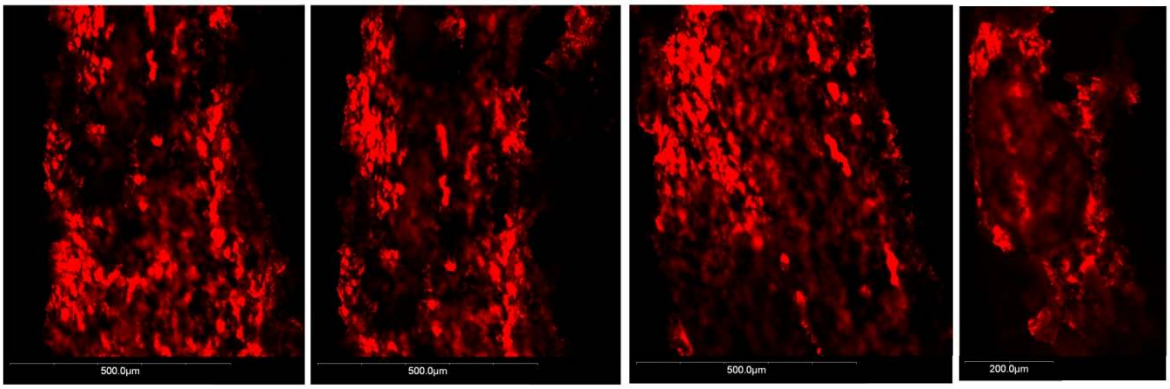

Figure 5.18: CLSM images of S-Thin samples

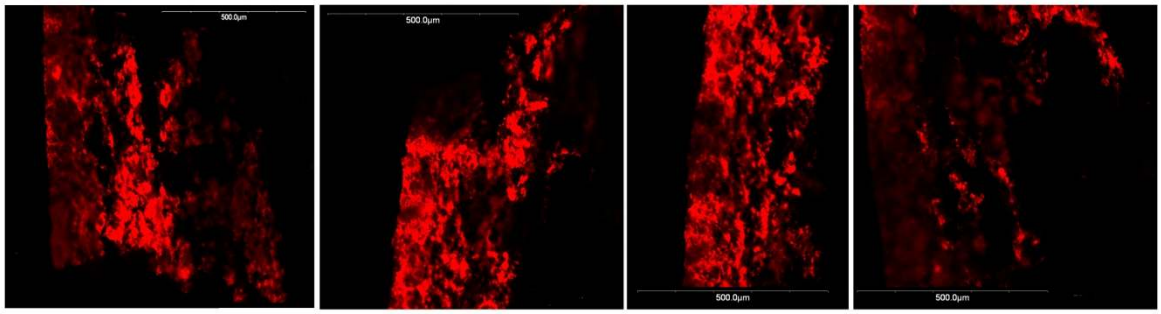

Figure 5.19: CLSM images of F-Thin samples

The thicknesses of the oil layers was measured through image analysis, as explained in section 4.8.4. Results are shown in Table 5.3. In order to better understand oil absorption in thick products, both oil layers were added as shown in the Table. Double layer formation may be due to the effect of vapor escape in structure development. Since thick products are submitted to longer frying times, there could be a separation of the crust due the longer time needed to achieved the a certain dehydration level.

Table 5.3: Crust Thickness of different samples and layers estimated from CLSM images (mean values ± standard deviation, n=4). On the left column the measure of a single oil layer is measured, which is total thickness for thin products. For thick products total thickness is the sum of layers 1 and 2 which is presented on the "Sum of layers column".

Sample	Crust thickness (μm)		
S-Thin	270	±	13
F-Thin	319	±	12
S-Thick layer1	146	±	19
S-Thick layer2	193	±	14
Sum of layers	339	±	15
F-Thick layer1	148	±	23
F-Thick layer2	221	±	12
Sum of layers	369	±	14

All values of crust thickness were significantly different ($p<0.05$). It can be noticed that, altogether, thick products contained a ticker crust than thin products, which is consistent with oil uptake measurements. Also, it can be seen that fast-frozen products had a larger crust than slow-frozen ones. This is in accordance with total oil-uptake values presented in section 5.1, supporting the hypothesis that a greater collapse and packing of the structure may occur in slow-frozen products, which may preclude oil penetration. On the other hand fast -frozen products presented a thicker crust (and oil) because of a better preserved structure, due to the impossibility to form ice crystals at high freezing rates. Similar results were observed by Moreno and Bouchon (2008) in a freeze drying process, where the abrupt freezing of foods preserved the structure and increased oil absorption.

6 CONCLUSION

Overall, it can be concluded that through the experimental set-up developed throughout this thesis, it was possible to analyze, through a reproducible procedure, the effect of the freezing rate on the microstructure of gluten and starch formulated dough during deep-fat frying and associated transport phenomena, particularly oil absorption.

Specifically, it was possible to conclude that slow frozen products took a longer frying time to reach the same moisture content than fast frozen products, probably because bigger ice crystals where formed, which are harder to melt. This in turn, resulted in different fried-dough microstructures, which were adequately characterized –non-invasively– through confocal laser scanning microscopy. Fast frozen products melted faster and had higher heating rates during the deep-fat frying process. This was related to faster crust formation and a better conservation of food structure, which allow better oil infiltration after deep-fat frying. On the other hand, slow frozen products were believed to suffer a microstructure collapse and a consequent packing of the external layers, which lead to lower oil permeability.

More dehydrated products had increased amounts of total oil, because water migration left space for oil deposition within the structure. This was reflected by a good linear correlation between moisture loss and oil uptake for each product category. However, an overall correlation could not be established, since different product categories absorbed different amounts of oil for a given moisture loss. To get a better understanding of this behavior, total oil was divided into two fractions: penetrated oil and surface oil, whose distribution depended on the competition between drainage and suction of oil during the cooling process. Penetrated oil also increased with longer frying times, as total oil did. No significant differences between thin and thick products were observed, meaning that the mechanics of oil penetration were mostly related to the structure caused by the freezing process. Penetrated oil was in average 52% higher on fast frozen products than in slow frozen ones. As penetrated oil represented the greatest part of total oil, the phenomenon behind oil absorption was basically the same, which

made the study on surface oil an important factor. Overall, differences in total oil absorption between thin and thick products were due to this oil fraction. These differences could be maybe attributed to differences in surface roughness, which may reduce oil drainage in thin samples, but further studies are needed to elucidate this hypothesis.

Generally, this works sets-up an initial basis to understand the relationship between freezing and deep-fat frying, and thus, represent a novel contribution in the field of food product design, to meet new consumer's demands.

REFERENCES

Aguilera, J. M. (2005). Why food microstructure? *Journal of Food Engineering, 67*, 3-11.

AOAC. (1995). Official Methods of Analysis: 16th ed. Association of Official Analytical Chemists, Washington, DC, Unites States.

Blumenthal, M. M. (1991). A new look at the chemistry and physics of deep-fat frying. *Food Technology, 45*, 68-71.

Bouchon, P., & Aguilera, J. M. (2001). Microstructural analysis of frying potatoes. *International Journal of Food Science and Technology, 36*, 669-676.

Bouchon, P., Aguilera, J. M., & Pyle, D. L. (2003). Structure-oil absorption kinetics relationships during deep-fat frying. *Journal of Food Science, 68*(2711-2716).

Bouchon, P., & Pyle, D. L. (2004). Studying Oil Absorption in Restructured Potato Chips. *Journal of Food science, 69*(3), 115-122.

Carbonell, S., Oliveira, J. C., & Kelly, A. L. (2006). Effect of pretreatments and freezing rate on the firmness of potato tissue after a freeze–thaw cycle. *International Journal of Food Science and Technology, 41*, 757-767.

Carra, L., Rodasb, M., Della Torreb, J., & Tadinia, C. (2006). Physical, textural and sensory characteristics of 7-day frozen part-baked French bread. *Lebensmittel–Wissenschaft und Technologie, 39*, 540-547.

Ceballos, A. M., Giraldo, G. I., & Orrego, C. E. (2012). Effect of freezing rate on quality parameters of freeze dried soursop fruit pulp. *Journal of Food Engineering, 111*(2), 360-365.

Delgado, A. E., & Sun, D.-W. (2001). Heat and mass transfer models for predicting freezing processes – a review. *Journal of Food Engineering, 47*(3), 157-174.

Dueik, V., & Bouchon, P. (2011). Development of healthy low-fat snacks: understanding the mechanisms of quality changes during atmospheric and vacuum frying. *Food Reviews International, 27*(4), 408-432.

Eliasson, A. C., & Gudmundsson, M. (1996). Starch: physichochemical and functional aspects. *Carbohydrates in food* (pp. 431-503). New York.

Fuchigami, M., Miyazaki, K., & Hyakumoto, N. (1995). Frozen Carrots Texture and Pectic Compotients as Affected by Low-Temperature-Blanching and Quick Freezing. *Journal of Food science, 60*(1), 132-136.

Gamble, M., Rice, P., & Selman, J. (1987). Relationship between oil uptake and moisture loss during frying of potato slices from c. v. Record U.K. tubers. *International Journal of Food Science & Technology, 22*(3), 233-241.

□□□í□, M. A., Ferrero, C., Bértola, N., Martino, M., & Zaritzky, N. (2002). Edible coatings from cellulose derivatives to reduce oil uptake in fried products. *Innovative Food Science & Emerging Technologies, 3*(4), 391-397.

Gazmuri, A. M., & Bouchon, P. (2009). Analysis of wheat gluten and starch matrices during deep-fat frying. *Food Chemistry, 115*(3), 999-1005.

Gómez, M., Ruiz, E., & Oliete, B. (2011). Effect of batter freezing conditions and resting time on cake quality. *Food Science and Technology, 44*, 911-916.

Grandison, A. S. (2012). Postharvest Handling and Preparation of Foods for Processing. In J. G. Brennan & A. S. Grandison (Eds.), *Food processing handbook*: John Wiley & Sons.

Hartel, R. W. (2001). *Crystallization in foods*. Gaithersburg: Aspen Publishers Inc.

Kiani, H., & Sun, D.-W. (2011). Water crystallization and its importance to freezing of foods: A review. *Trends in Food Science & technology, 22*(8), 407-426.

Kochs, M., Körber, C. H., Heschel, I., & Nunner, B. (1991). The influence of the freezing process on vapour transport during sublimation in vacuum-freeze-drying. *International Journal of Heat and Mass Transfer, 34*, 2395-2408.

Lee, J., & Cheng, Y. (2006). Critical freezing rate in freeze drying nanocrystal dispersions. *Journal of Controlled Release, 111*(1–2), 185-192.

Llorca, E., Hernando, I., Pérez-Munuera, I., Fiszman, S., & Luch, M. (2001). Effect of frying on the microstructure of frozen battered squid rings. *European Food Research Technology, 213*, 448-455.

Llorca, E., Hernando, I., Pérez-Munuera, I., Quiles, A., Larrea, V., & Lluch, M. (2007). Protein breakdown during the preparation of frozen batter-coated squid rings. *European Food Research Technology, 225*, 807-813.

Malkki, Y., Puolakka, L., & Paakkanen, J. (1974). Effect of freezing and thawing conditions on the rheological properties of bakery products. *Deutsche Gesellschaft fuer Chemisches Apparatewesen, 77*(1505-1536), 165-175.

Marques, L. G., Ferreira, M. C., & Freiré, J. T. (2007). Freeze-drying acerola (Malpigltiaglabra L.). *Chemical Engineering Processes, 46*, 451-457.

Mellema, M. (2003). Mechanism and reduction of fat uptake in deep-fat fried foods. *Trends in Food Science & technology, 14*(9), 364-373.

Meziani, S., Ioannou, I., Jasniewski, J., Belhaj, N., Muller, J.-M., Ghoul, M., & Desobry, S. (2012). Effects of freezing treatments on the fermentative activity and gluten network integrity of sweet dough. *LWT - Food Science and Technology, 46*(1), 118-126.

Meziani, S., Jasniewski, J., Gaiani, C., Ioannou, I., Muller, J.-M., Ghoul, M., & Desobry, S. (2011). Effects of freezing treatments on viscoelastic and structural behavior of frozen sweet dough. *Journal of Food Engineering, 107*(3–4), 358-365.

Moreira, R. G., Sun, X., & Chen, Y. (1997). Factors affecting oil uptake in tortilla chips in deep-fat frying. *Journal of Food Engineering, 31*, 485-498.

Moreno, C. (2012). *Microstructure and transport phenomena in deep-fat fried formulated products*. Doctoral thesis.

Moreno, C., & Bouchon, P. (2008). A Different Perspective to Study the Effect of Freeze, Air, and Osmotic Drying on Oil Absorption during Potato Frying. *Journal of Food science, 73*(3), E122-E128.

Moreno, C., & Bouchon, P. (2013). Microstructural characterization of deep-fat fried formulated products using confocal scanning laser microscopy and a non-invasive double staining procedure. *Journal of Food Engineering, 118*(2), 238-246.

Moreno, C., Brown, C. A., & Bouchon, P. (2010). Effect of food surface roughness on oil uptake by deep-fat fried products. *Journal of Food Engineering, 101*(2), 179-186.

Muse, M. R., & Hartel, R. W. (2004). Ice Cream Structural Elements that Affect Melting Rate and Hardness. *Journal Of Dairy Science, 87*, 1-10.

O'Brien, F. J., Harley, B. A., Yannas, I. V., & Gibson, L. (2004). Influence of freezing rate on pore structure in freeze-dried collagen-GAG scaffolds. *Biomaterials, 25*(6), 1077-1086.

Pardo, J., & Niranjan, K. (2006). Freezing. In J. G. Brennan (Ed.), *Food Processing Handbook*: Wiley-VCH.

Pedreschi, F., Aguilera, J. M., & Arbildua, J. J. (1999). CLSM study of oil location in fried potato slices. *Microscopy and Analysis, 37*, 21-22.

Petzold, G., & Aguilera, J. M. (2009). Ice morphology: fundamentals and technological applications in foods. *Food Biophysics, 4*(4), 378-396.

Pinthus, E. J., Weinberg, P., & Saguy, I. S. (1995). Oil uptake in deep fat frying as affected by porosity. *Journal of Food Science, 60*(4), 767-769.

Plank, R. (1963). *El empleo del frío en la industria de la alimentación*. Barcelona: Editorial Reverté.

Rahman, M. S. (2007). *Handbook of food preservation*: CRC Press.

Rahman, M. S. (2008). Freezing Point: Measurment, Data, and Prediction. In M. S. Rahman (Ed.), Food Properties Handbook.

Rahman, M. S., Guizani, N., Al-Khaseibi, M., Ali Al-Hinai, S., Al-Maskri, S. S., & Al-Hamhami, K. (2002). Analysis of cooling curve to determine the end point of freezing. *Food Hydrocolloids, 16*(6), 653-659.

Roos, Y. (2010). Glass transition temperature and its relevance in food processing. *Annual Reviews of Food Science and Technology, 1*, 469-496.

Sun, D. W. (2011). *Handbook of frozen food processing and packaging*: CRC Press.

Tressler, D. K., Van Arsdel, W. B., & Copley, M. J. (1968). *The freezing preservation of foods*. Westport, Conn: The AVI Publishing Compagny.

Ufheil, G., & Escher, F. (1996). Dynamics of oil uptake during deep-fat frying of potato slices. *Lebensmittel–Wissenschaft und Technologie, 29*, 640-644.

Veraverbeke, W. S., & Delcour, J. A. (2002). Wheat protein composition and properties of wheat glutenin in relation to breadmaking functionality. *Critical Reviews in Food Science and Nutrition, 42*(3), 179-208.

Wathen, B., Kuiper, M., Walker, V., & Jia, Z. (2004). New Simulation Model of Multicomponent Crystal Growth And Inhibition. *Chemistry – A European Journal, 10*(7), 1598-1605.86

APPENDIXES

APPENDIX A: MOISTURE AND OIL MEASURMENTS OF DIFFERENT PRODUCTS

A.1 30% Moisture Content Products

Slow-freezing Thick

Surface Oil

	M0	M1	B0	B1	Solidos	SO	%SO	W	%W
RG1	99,8514	82,8205	107,2404	107,7698	58,7026	0,5294	0,90%	17,8094	30,34 %
RG2	99,7654	81,8145	106,227	106,7426	58,6521	0,5156	0,88%	17,1086	29,17 %
RG3	95,9554	79,1859	135,0086	135,5387	56,4122	0,5301	0,94%	16,7714	29,73 %

Soxhlet

	B0	B1	P0	P1	%PO	PO	%TO
RG1	135,7643	136,707	31,6809	41,2567	9,84%	5,77904477	10,75 %
RG2	105,6026	106,5208	31,2223	40,9465	9,44%	5,53817678	10,32 %
RG3	107,1411	107,8114	30,2103	37,1203	9,70%	5,47222634	10,64 %

Fast-freezing Thick

Surface Oil

	M0	M1	B0	B1	Solidos	SO	%SO	W	%W
RG1	97,1562	82,075	106,2547	106,6564	57,1181	0,4017	0,70%	17,2303	30,17 %
RG2	97,4323	81,7591	103,8391	104,3194	57,2804	0,4803	0,84%	16,8585	29,43 %
RG3	93,0235	78,5087	105,9202	106,2988	54,6885	0,3786	0,69%	16,4000	29,99 %

Soxhlet

	B0	B1	P0	P1	%PO	PO	%TO
RG1	135,7661	137,0586	31,6865	41,7652	12,82%	7,32487156	13,53 %
RG2	105,6088	106,7843	31,2243	40,6549	12,46%	7,13986045	13,30 %
RG3	107,1456	107,9865	30,2212	36,7521	12,88%	7,04153682	13,57 %

Slow-freezing Thin

Surface Oil

	M0	M1	B0	B1	Solidos	SO	%SO	W	%W
DL1	48,6693	40,9148	107,2391	107,7871	28,6127	0,548	1,92%	8,8962	31,09 %
DL2	49,085	40,8871	125,0588	125,588	28,8571	0,5292	1,83%	8,5601	29,66 %
DL3	50,3861	42,2122	105,9208	106,4826	29,6220	0,5618	1,90%	8,9370	30,17 %

Soxhlet

	B0	B1	P0	P1	%PO	PO	%TO
DL1	135,8661	136,8833	31,6447	41,8288	9,99%	2,8578686	11,90 %
DL2	105,5993	106,588	31,2165	40,9184	10,19%	2,9407628	12,02 %
DL3	107,1403	107,8076	30,2195	36,6136	10,44%	3,091405	12,33 %

Fast-freezing Thin

Surface Oil

	M0	M1	B0	B1	Solidos	SO	%SO	W	%W
DR1	47,3473	40,235	103,8401	104,2112	27,8355	0,3711	1,33%	8,3865	30,13 %
DR2	48,8234	41,2469	106,6525	106,9976	28,7033	0,3451	1,20%	8,5276	29,71 %
DR3	50,1698	42,5417	105,8944	106,2892	29,4948	0,3948	1,34%	8,7679	29,73 %

Soxhlet

	B0	B1	P0	P1	%PO	PO	%TO
DR1	125,0586	126,6049	30,2972	42,1158	13,08%	3,64188644	14,42 %
DR2	103,8318	105,0312	33,5566	42,9347	12,79%	3,67096856	13,99 %
DR3	107,1437	108,0555	30,218	37,1418	13,17%	3,88419391	14,51 %

A.2 40% Moisture Content Products

Slow-freezing Thick

Dryweigh t

	P0	P1	P2		
M1	37,2892	41,9638	40,0267	0,4143884	%W
M2	30,9075	34,4807	33,0028	0,41360685	41,30%
M3	29,873	33,4859	32,0011	0,4109718	

Surface Oil

	M0	M1	B0	B1	Solidos	SO	%SO	W	%W
RG1	104,6644	90,8583	105,9374	106,4875	61,4392	0,5501	0,90%	24,5949	40,03%
RG2	108,8584	95,6959	107,2805	107,8408	63,9011	0,5603	0,88%	26,3254	41,20%
RG3	101,8873	89,6822	103,8415	104,3833	59,8090	0,5418	0,91%	24,7665	41,41%
RG4	105,5361	91,8973	125,0691	125,6327	61,9509	0,5636	0,91%	24,7318	39,92%

Soxhlet

	B0	B1	P0	P1	%PO	PO	%TO
RG1	105,954	106,4943	30,299	38,0656	6,96%	4,27414495	7,85%
RG2	106,3294	106,7803	33,5575	39,4268	7,68%	4,90910253	8,56%
RG3	105,6191	106,161	30,22	37,3199	7,63%	4,56492032	8,54%
RG4	107,2995	107,8514	31,2182	38,5694	7,51%	4,65103305	8,42%

Fast-freezing Thick

Dryweigh t

	P0	P1	P2		
M1	37,2862	41,3357	39,6829	0,40814915	%W
M2	30,9088	34,6703	33,123	0,41135185	40,97%
M3	29,8732	33,0736	31,7623	0,40973003	

Surface Oil

	M0	M1	B0	B1	Solidos	SO	%SO	W	%W
RG1	101,472	90,2048	135,867	136,3165	59,894	0,4495	0,75%	23,919	39,94

	3				7			3	%
RG2	101,4431	90,4675	135,0602	135,5327	59,8774	0,4725	0,79%	23,8164	39,78 %
RG3	101,3201	90,1561	107,1736	107,5944	59,8048	0,4208	0,70%	24,0372	40,19 %
RG4	99,4202	89,8139	106,668	107,0989	58,6834	0,4309	0,73%	24,2076	41,25 %

Soxhlet

	B0	B1	P0	P1	%PO	PO	%TO
RG1	135,0434	135,877	30,1287	38,5323	9,92%	5,94128633	10,67 %
RG2	105,9777	106,7644	33,5568	41,0325	10,52%	6,30115907	11,31 %
RG3	106,3097	107,0721	30,2977	38,0345	9,85%	5,89328945	10,56 %
RG4	106,6554	107,665	31,2175	40,3436	11,06%	6,49201323	11,80 %

Slow-freezing Thin

Dryweigh t

	P0	P1	P2		
M1	37,2886	40,8391	39,3734	0,4128151	%W
M2	30,91	35,6189	33,6795	0,4118584	41,21%
M3	29,8756	34,9063	32,8354	0,41165245	

Surface Oil

	M0	M1	B0	B1	Solidos	SO	%SO	W	%W
DL1	50,5781	44,3128	135,8684	136,4179	29,6899	0,5495	1,85%	11,7636	39,62 %
DL2	49,8221	43,8971	107,1598	107,697	29,2461	0,5372	1,84%	11,8153	40,40 %
DL3	51,3698	45,3124	103,8526	104,396	30,1546	0,5434	1,80%	12,1693	40,36 %
DL4	48,6005	43,0644	125,0851	125,5828	28,5290	0,4977	1,74%	11,7188	41,08 %

Soxhlet

	B0	B1	P0	P1	%PO	PO	%TO
DL1	107,2374	107,827	30,2991	37,8777	7,78%	2,30981517	9,63%
DL2	135,8758	136,5102	30,2215	38,2938	7,86%	2,29844512	9,70%
DL3	105,6083	106,391	33,5573	43,2101	8,11%	2,44509721	9,91%

DL4	107,1511	107,9063	31,217	40,5083	8,13%	2,31884898	9,87%

Fast-Freezing Thin

Dryweigh t

	P0	P1	P2		
M1	37,2889	41,1728	39,568	0,41319292	%W
M2	30,9091	34,498	33,0134	0,41366435	41,36%
M3	29,8748	34,1251	32,3651	0,41408842	

Surface Oil

	M0	M1	B0	B1	Solidos	SO	%SO	W	%W
DR1	52,6641	47,1113	107,2216	107,6029	30,9144	0,3813	1,23%	12,2458	39,61%
DR2	51,0731	45,3093	135,8852	136,2639	29,9805	0,3787	1,26%	11,7895	39,32%
DR3	51,8557	46,3791	105,6103	105,9638	30,4399	0,3535	1,16%	12,4012	40,74%
DR4	49,5144	44,2738	107,1571	107,574	29,0655	0,4169	1,43%	11,7212	40,33%

Soxhlet

	B0	B1	P0	P1	%PO	PO	%TO
DR1	105,9259	106,737	30,2965	37,3207	11,55%	3,56975515	12,78%
DR2	125,0616	125,8252	30,2188	37,4619	10,54%	3,16067533	11,81%
DR3	103,8222	104,6904	33,5561	41,8549	10,46%	3,1845437	11,62%
DR4	106,6313	107,3439	31,2158	37,9619	10,56%	3,07022917	12,00%

A.3 50% Moisture Content Products

Slow-freezing Thick

Surface Oil

	M0	M1	B0	B1	Solidos	SO	%SO	W	%W
RG1	99,8514	91,9705	107,2404	107,7198	58,7026	0,4794	0,82%	29,2513	49,83%
RG2	99,7654	92,2145	106,227	106,7426	58,6521	0,5156	0,88%	29,4508	50,21%
RG3	97,9554	90,7859	135,0086	135,4887	57,5880	0,4801	0,83%	29,2984	50,88%

Soxhlet

	B0	B1	P0	P1	%PO	PO	%TO
RG1	135,7643	136,3413	31,6809	41,2567	6,03%	3,53718981	6,84%
RG2	105,6026	106,1988	31,2223	40,9465	6,13%	3,59601502	7,01%
RG3	107,1411	107,5514	30,2103	37,1203	5,94%	3,41944255	6,77%

Fast-freezing Thick

Surface Oil

	M0	M1	B0	B1	Solidos	SO	%SO	W	%W
RG1	97,1426	92,075	106,2547	106,6564	57,1101	0,4017	0,70%	30,0725	52,66%
RG2	97,65711	91,7591	103,8391	104,2194	57,4126	0,3803	0,66%	29,4800	51,35%
RG3	97,0235	90,5087	105,9202	106,3144	57,0401	0,3942	0,69%	28,3502	49,70%

Soxhlet

	B0	B1	P0	P1	%PO	PO	%TO
RG1	135,7661	136,5586	31,6865	41,7652	7,86%	4,49063685	8,57%
RG2	105,6088	106,3457	31,2243	40,6549	7,81%	4,48617861	8,48%
RG3	107,1456	107,6865	30,2212	36,7521	8,28%	4,72415725	8,97%

Slow-freezing Thin

Surface Oil

	M0	M1	B0	B1	Solidos	SO	%SO	W	%W
DL1	49,6923	46,1105	134,9954	135,4489	29,2141	0,4535	1,55%	14,6724	50,22%
DL2	48,7941	45,5463	105,9106	106,3803	28,6861	0,4697	1,64%	14,6263	50,99%
DL3	49,3829	46,0151	125,0512	125,5151	29,0322	0,4639	1,60%	14,6243	50,37%

Soxhlet

	B0	B1	P0	P1	%PO	PO	%TO
DL1	135,8661	136,4833	31,6447	41,8288	6,06%	1,77049955	7,61%
DL2	105,5993	106,196	31,2165	40,9184	6,15%	1,76429018	7,79%
DL3	107,1403	107,5576	30,2195	36,6136	6,53%	1,89473733	8,12%

Fast-freezing Thin

Surface Oil

	M0	M1	B0	B1	Solidos	SO	%SO	W	%W
DR1	49,5046	47,0552	135,0124	135,365	29,1038	0,3526	1,21%	15,0654	51,76%
DR2	48,1231	46,0344	105,9215	106,2492	28,2916	0,3277	1,16%	15,0904	53,34%

DR3	47,2668	44,8675	106,6316	106,9379	27,7882	0,3063	1,10%	14,5584	52,39%

Soxhlet

	B0	B1	P0	P1	%PO	PO	%TO
DR1	125,0586	126,0874	30,2972	42,1158	8,70%	2,53345933	9,92%
DR2	103,8318	104,6024	33,5566	42,9347	8,22%	2,32472294	9,38%
DR3	107,1437	107,6955	30,218	37,1418	7,97%	2,21460789	9,07%

APPENDIX B: FINAL RESULTS OF MOISTURE AND OIL CONTENT

B.1 Table of Oil and Moisture Contents: statistical analysis is presented with colors within same products. Same color represent no significant differences are present.

		SO		PO		TO		W	
30% W	S-Thick	0,91%	0,03%	9,66%	0,20%	10,57%	0,22%	29,75%	0,58%
	F-Thick	0,74%	0,08%	12,72%	0,22%	13,47%	0,14%	29,86%	0,38%
	S-Thin	1,88%	0,04%	10,16%	0,22%	12,04%	0,44%	30,35%	0,91%
	F-Thin	1,29%	0,08%	13,01%	0,20%	14,31%	0,28%	29,86%	0,24%
		SO		PO		TO		W	
40% W	S-Thick	0,90%	0,01%	7,44%	0,33%	8,34%	0,33%	40,64%	0,77%
	F-Thick	0,74%	0,04%	10,34%	0,57%	11,08%	0,58%	40,29%	0,66%
	S-Thin	1,81%	0,05%	7,97%	0,18%	9,78%	0,14%	40,36%	0,59%
	F-Thin	1,27%	0,12%	10,78%	0,51%	12,05%	0,51%	40,00%	0,65%
		SO		PO		TO		W	
50% W	S-Thick	0,84%	0,03%	6,03%	0,10%	6,87%	0,12%	50,31%	0,53%
	F-Thick	0,69%	0,02%	7,99%	0,26%	8,67%	0,26%	51,24%	1,48%
	S-Thin	1,60%	0,04%	6,25%	0,25%	7,84%	0,26%	50,53%	0,40%
	F-Thin	1,16%	0,05%	8,30%	0,37%	9,45%	0,43%	52,50%	0,79%

B.2 Oil distribution of different samples and moisture contents (mean values ± standard deviation, n=4).

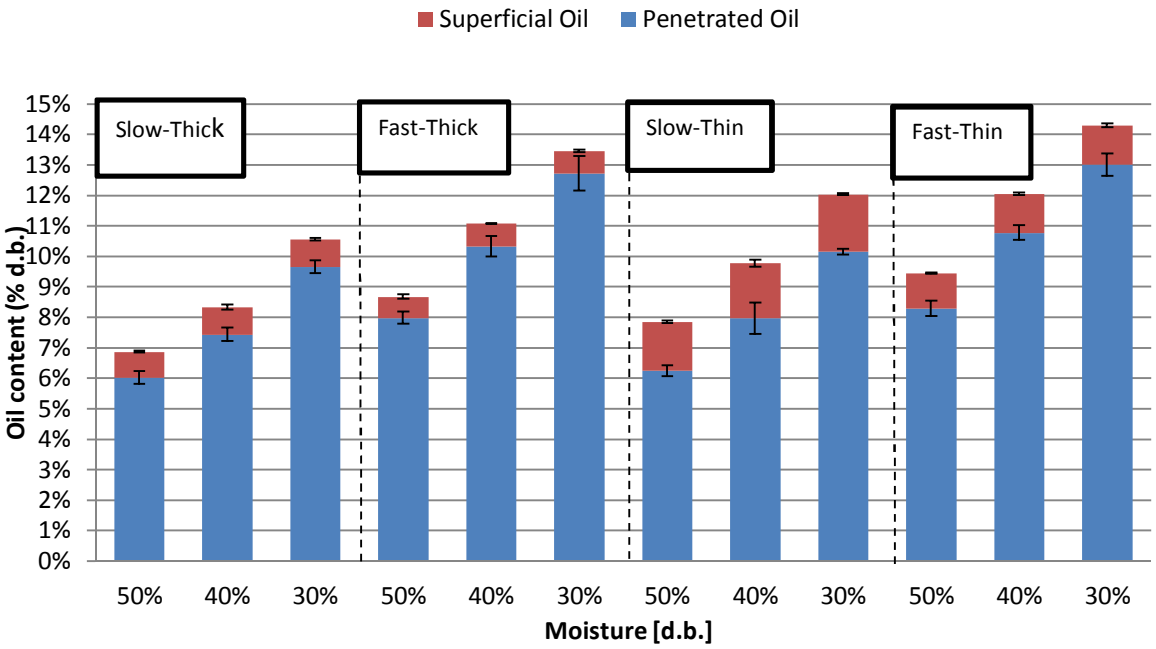

APPENDIX C: RESULTS OF PREELIMINARY IMAGE ANALYSIS

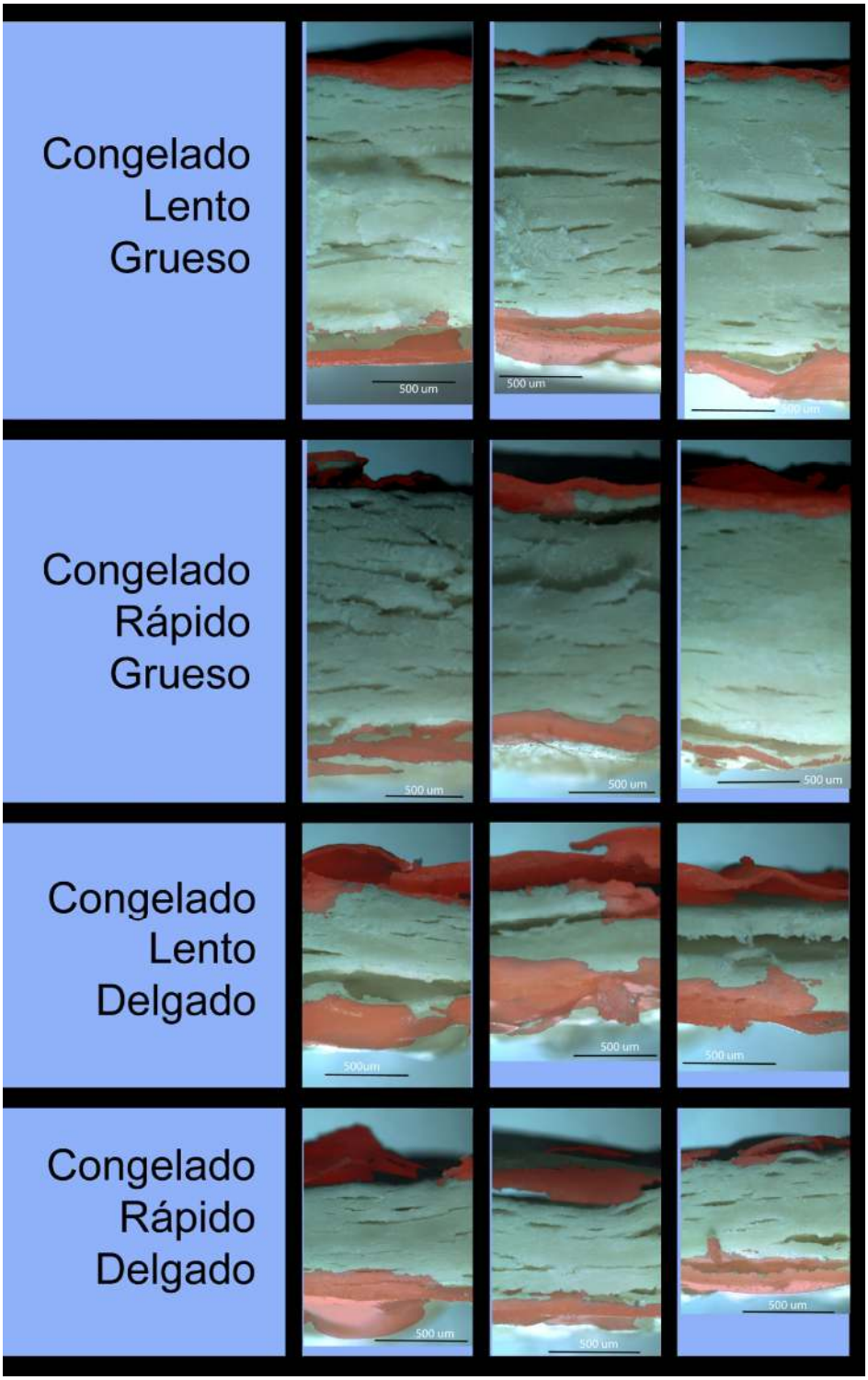

APPENDIX D: ORIGINAL IMAGES OF CLSM

D.1 Slow-Frozen Thin Products

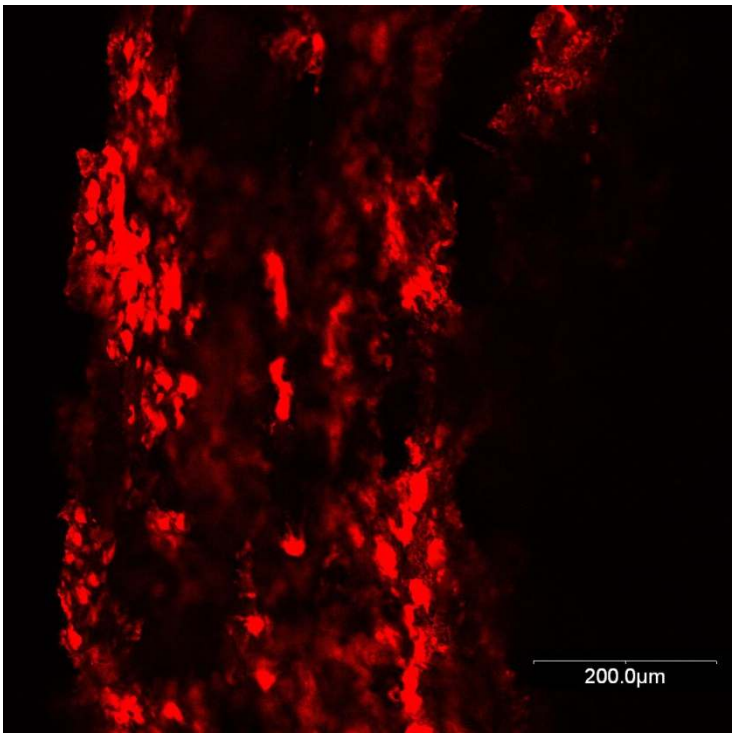

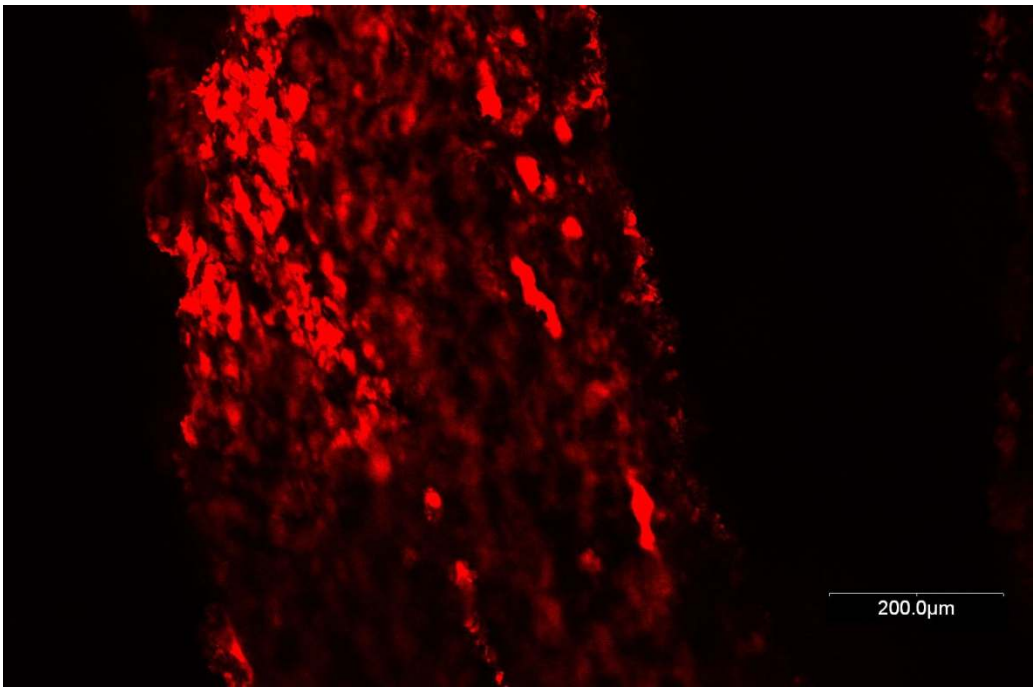

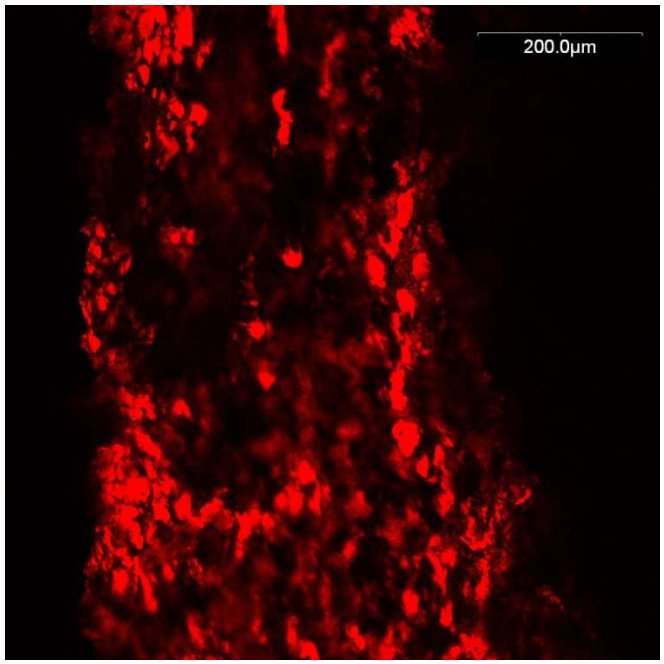
200.0µm

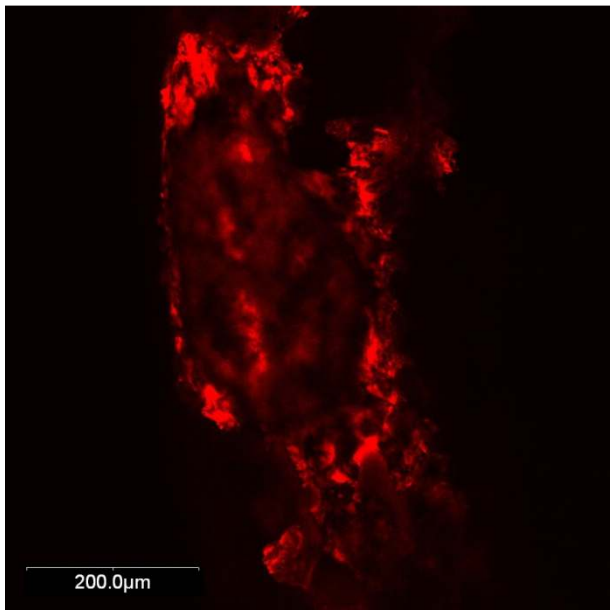
200.0µm

D.2 Fast-Frozen Thin Products

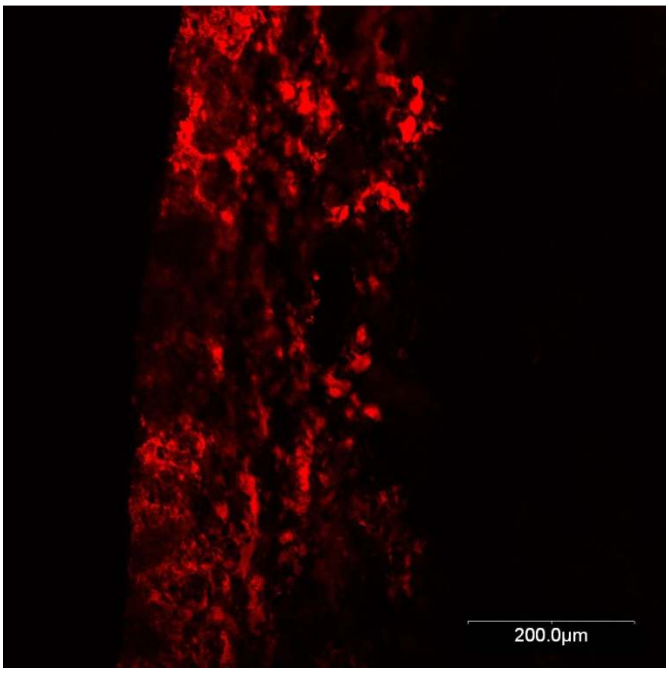

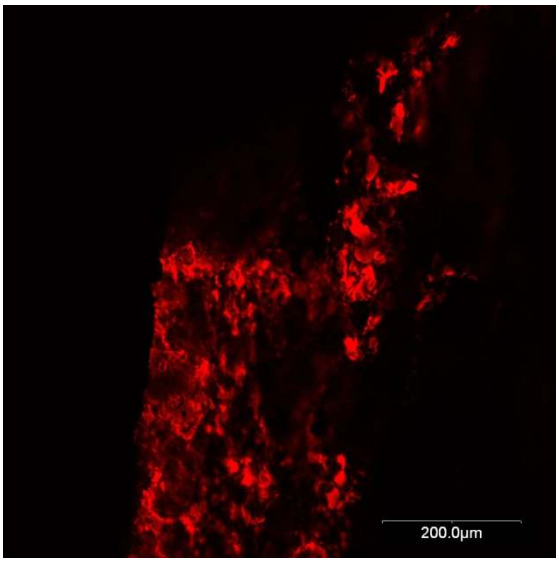

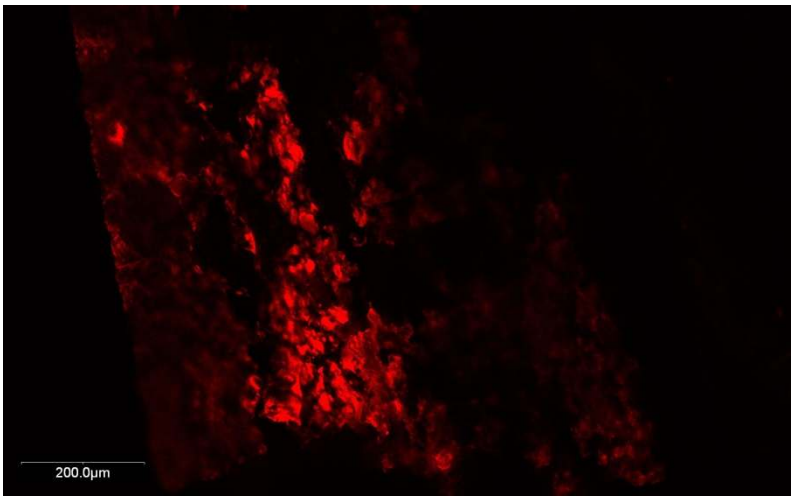
200.0µm

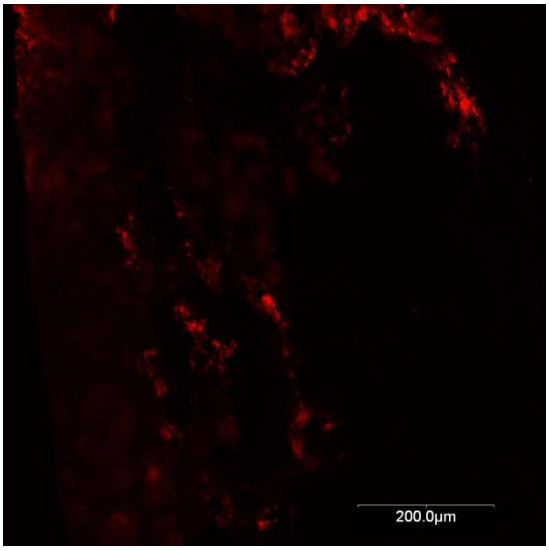
200.0µm

D.3 Slow-Frozen Thick Products

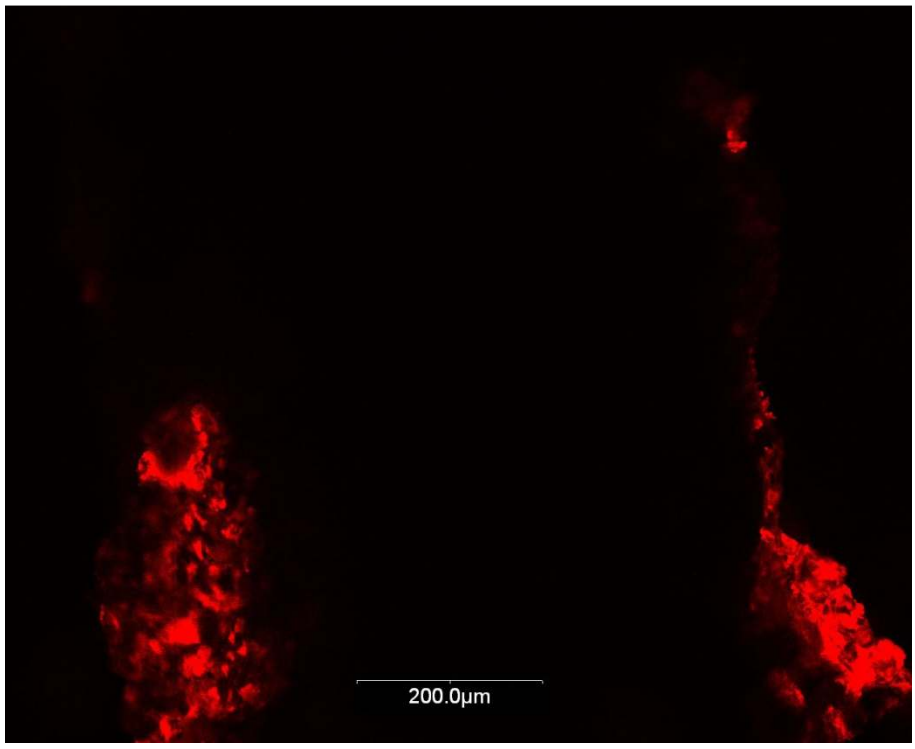

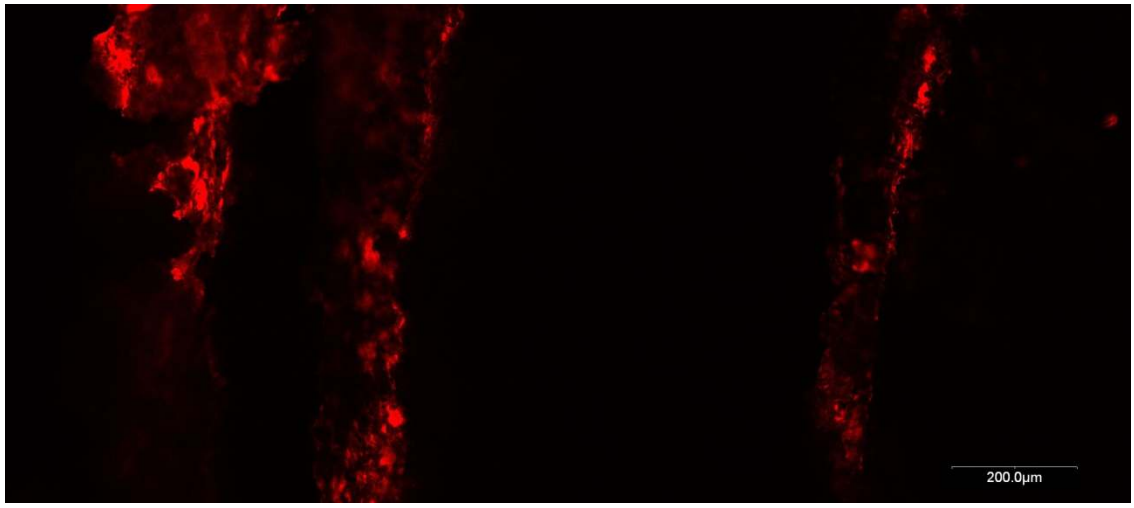

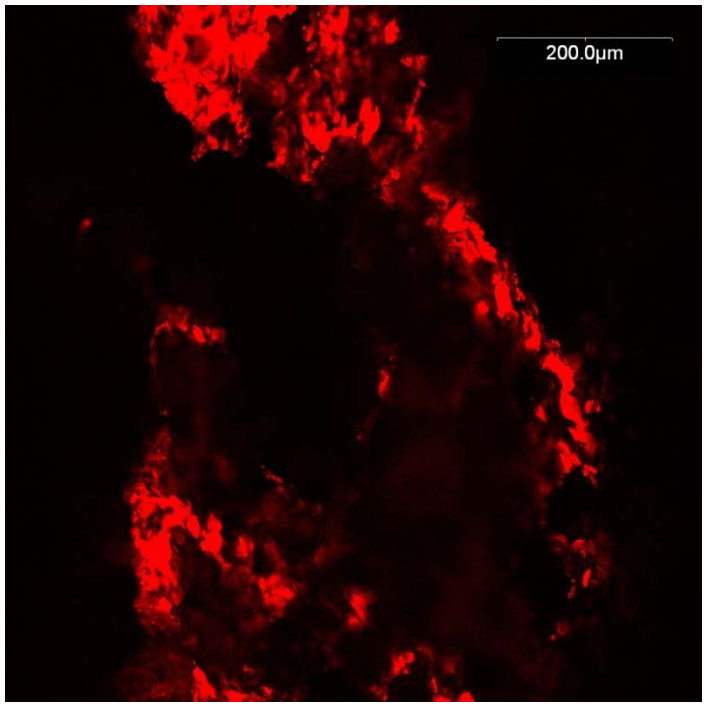
200.0µm

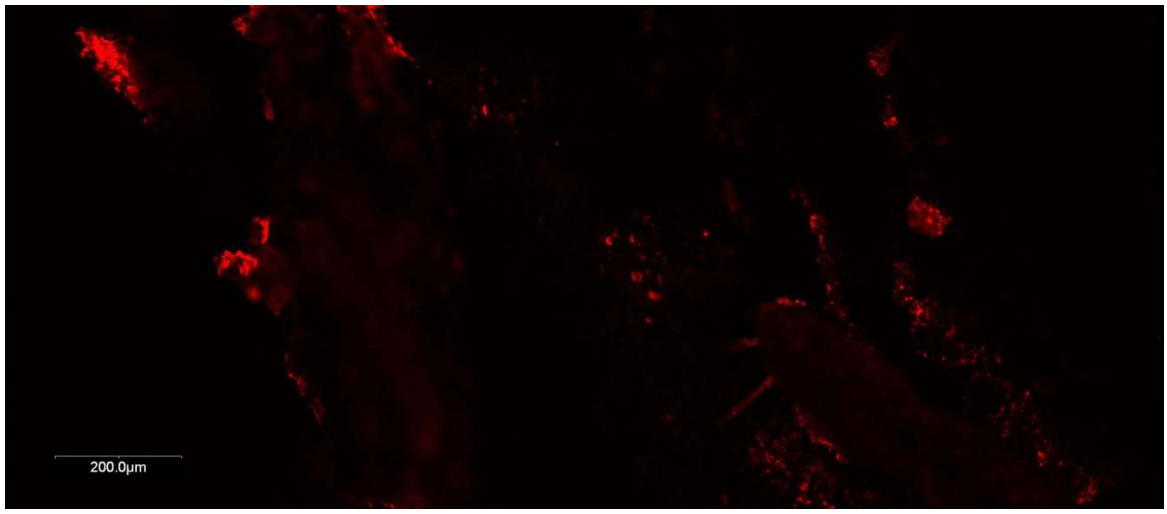
200.0µm

D.4 Fast-Frozen Thick Products

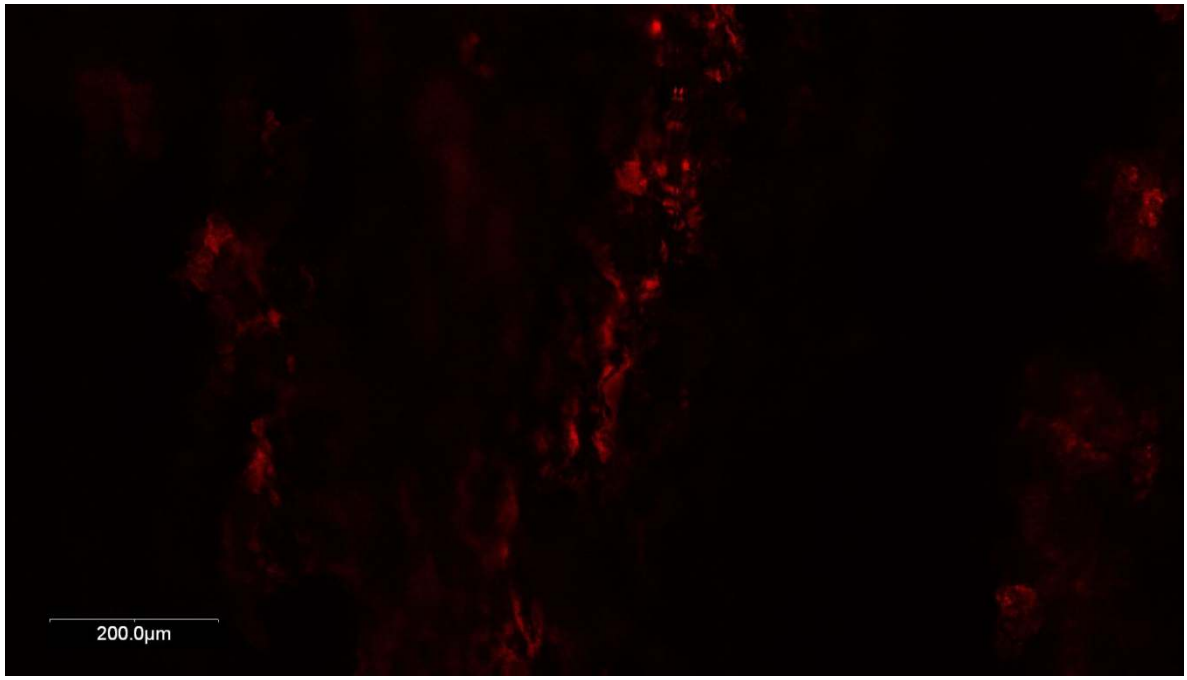

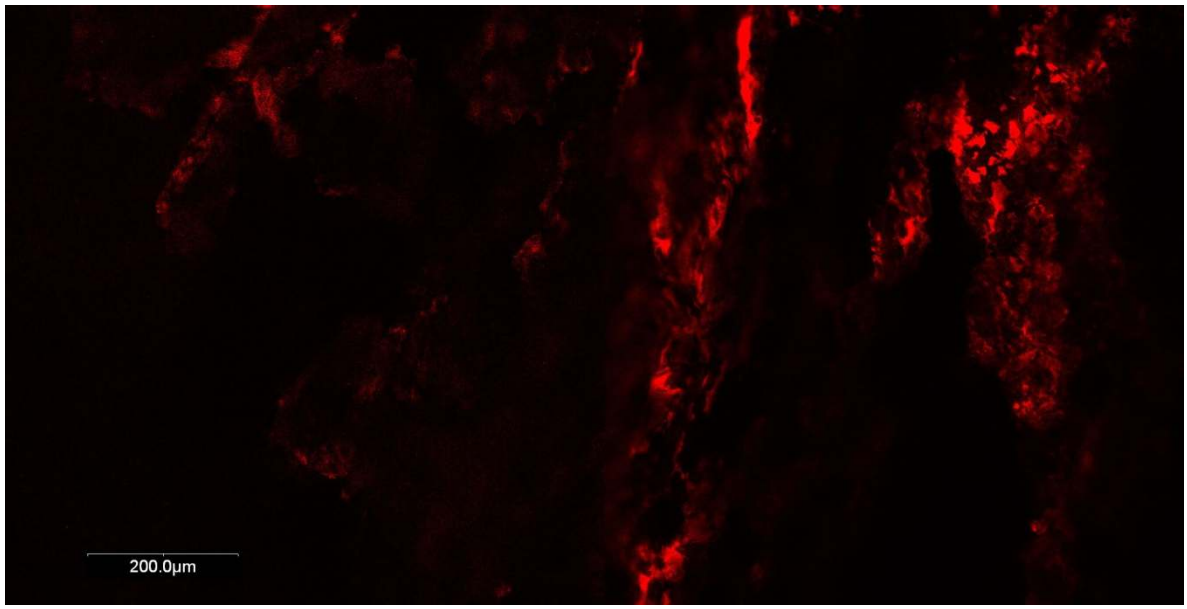

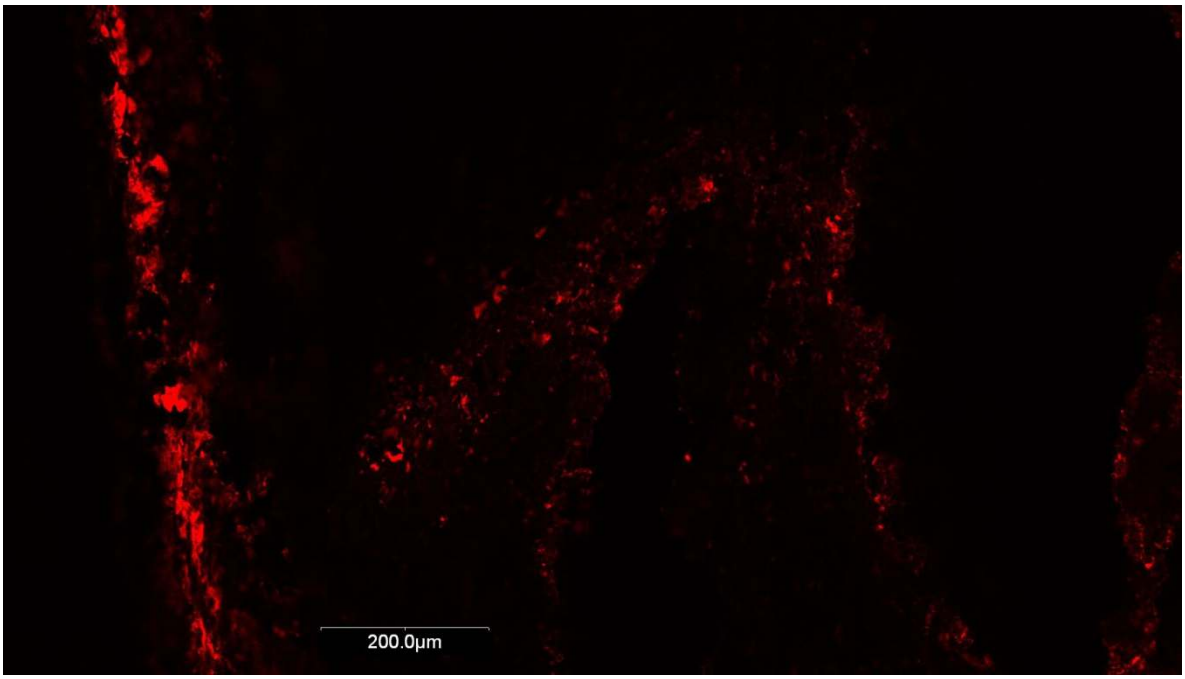
200.0µm

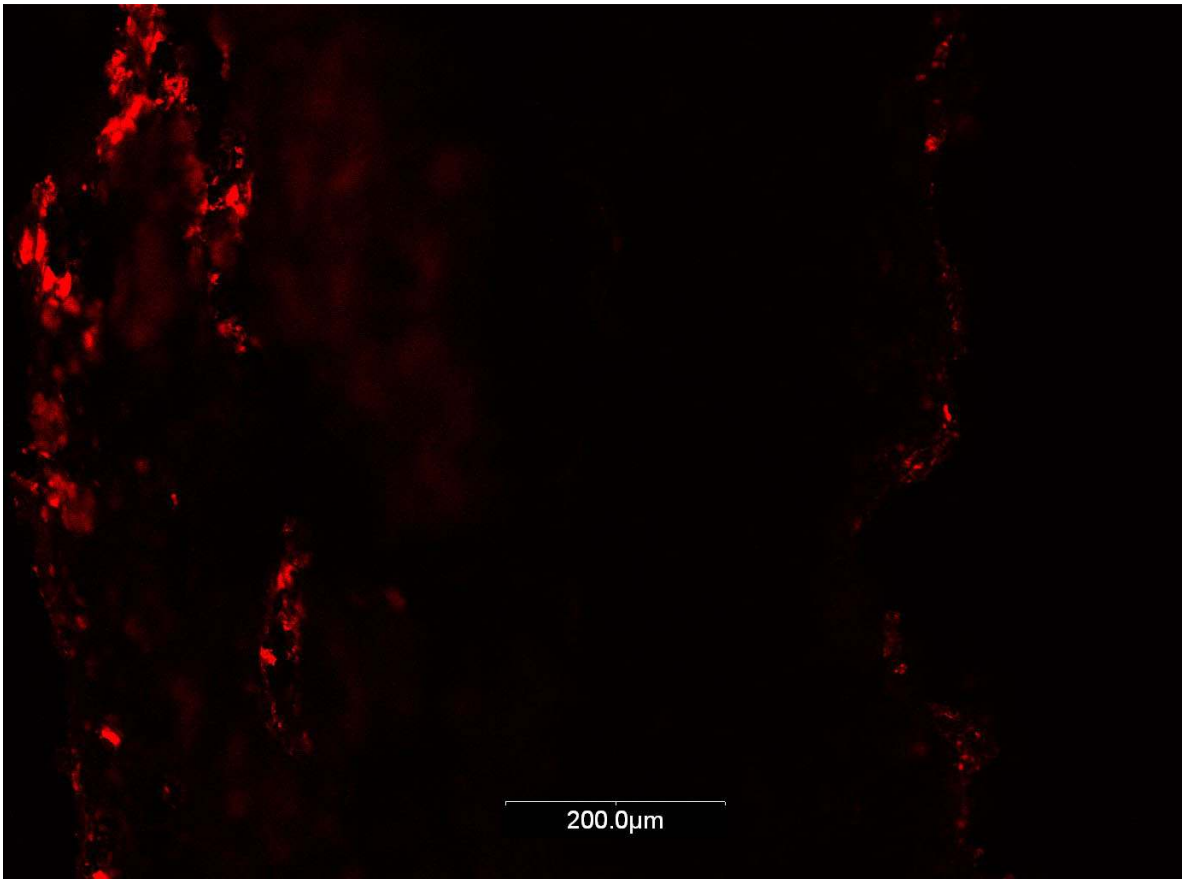
200.0µm